DEPARTMENT OF ECONOMICS
AND BUSINESS ECONOMICS
AARHUS UNIVERSITY

CREATES
Center for Research in Econometric Analysis of Time Series

The Extended Perturbation Method: New Insights on the New Keynesian Model

Martin M. Andreasen and Anders Kronborg

CREATES Research Paper 2017-14

Department of Economics and Business Economics
Aarhus University
Fuglesangs Allé 4
DK-8210 Aarhus V
Denmark

Email: oekonomi@au.dk
Tel: +45 8716 5515

The Extended Perturbation Method: New Insights on the New Keynesian Model*

Martin M. Andreasen†
Aarhus University and CREATES

Anders Kronborg‡
Danmarks Nationalbank and CREATES

March 27, 2017

Abstract

This paper introduces the extended perturbation method, which improves upon standard perturbation by removing approximation errors under perfect foresight. For the New Keynesian model, we show that standard perturbation generates explosive sample paths because it does not account for the upper bound on inflation as implied by Calvo pricing. In contrast, extended perturbation generates stable dynamics as it enforces this bound. Extended perturbation also adds to existing evidence on downward nominal wage rigidities in the New Keynesian model, as we only find support for this friction when using standard perturbation but not when using the more accurate extended perturbation approximation.

Keywords: Asymmetric wages, Extended Path, Perturbation method, Stable approximations.

JEL: C62, C68, E30

*We thank Rhys Bidder, Lawrence Christiano, Vasco Curdia, Wouter den Haan, Jens Iversen, Anders B. Kock, Eric Swanson, Allan Sørensen, Konstantinos Theodoridis, and Joris de Wind for useful comments and discussions. M. Andreasen greatly acknowledges financial support from the Danish e-Infrastructure Coorporation (DeIC). We also appreciate financial support to CREATES - Center for Research in Econometric Analysis of Time Series (DNRF78), funded by the Danish National Research Foundation.

†Corresponding author: Fuglesangs Allé 4, 8210 Aarhus V, Denmark, email: mandreasen@econ.au.dk; telephone +0045 87165982.

‡Havnegade 5, 1093 Copenhagen K, Denmark, email: akro@nationalbanken.dk.

1 Introduction

The solution to dynamic stochastic general equilibrium (DSGE) models is frequently approximated by the perturbation method to obtain higher-order Taylor series expansions of the policy function. The popularity of this approximation is mainly explained by its ability to i) preserve non-linearities in the model such as asymmetries, ii) improve parameter identification compared to a linearized solution, and iii) capture effects of uncertainty to explore determinants of risk premia and implications of uncertainty shocks (see An and Schorfheide (2007), Kim and Ruge-Murcia (2009), Fernández-Villaverde, Guerrón-Quintana, Rubio-Ramírez, and Uribe (2011), Rudebusch and Swanson (2012), among others).

Despite the widespread use of second- and third-order perturbation approximations, it is well known that they often generate explosive sample paths even when the corresponding linearized solution is stable. The perturbation approximation may also struggle to preserve key properties of the true solution such as monotonicity and convexity, as emphasized by Den Haan and De Wind (2012). These findings suggest that the second- and third-order perturbation approximations currently applied in the literature may not always be sufficiently accurate. Obtaining fourth- or even fifth-order expansions are often computationally infeasible and may even in some cases be insufficient to get an accurate approximation, as shown by Den Haan and De Wind (2012). A tractable alternative that preserves stability of the true solution, but not necessarily monotonicity, is to apply a pruning scheme, as proposed by Kim, Kim, Schaumburg, and Sims (2008) for models approximated to second order and extended to higher order by Den Haan and De Wind (2012), Andreasen, Fernandez-Villaverde, and Rubio-Ramirez (2013), and Lombardo and Uhlig (2014).

The contribution of the present paper is to improve the accuracy and stability of the perturbation approximation by combining it with the Extended Path of Fair and Taylor (1983). This is done based on a simple, yet powerful, decomposition of the policy function into i) a deterministic component under perfect foresight and ii) a stochastic component containing the effects of uncertainty. The perturbation method is currently applied to approximate *both* parts of the policy function, although the perfect foresight component may be approximated with arbitrary precision by the

Extended Path. Based on this observation, we propose to compute the perfect foresight component by the Extended Path, whereas the stochastic part of the policy function remains approximated by standard perturbation. We name this combined solution procedure the extended perturbation method, which improves accuracy and stability of standard perturbation by removing approximation errors under perfect foresight. The approximation order in the extended perturbation method is thus determined by the order of the polynomial used to approximate the stochastic part of the policy function.

For a second-order approximation, we show that extended perturbation always gives a stable solution without explosive sample paths, provided the model is stable under perfect foresight. This result does not generalize beyond second order and we therefore present a stability test to numerically evaluate if a given approximation is stable.

Using a standard New Keynesian model with Calvo pricing, we then show that extended perturbation achieves higher accuracy than standard perturbation when using third-order approximations. We also find that extended perturbation is stable even when standard perturbation explodes. To understand this striking difference, we use our stability test to locate the critical state configurations that lead to explosive dynamics. This analysis reveals that standard perturbation is unable to account for the upper bound on inflation induced by the Calvo pricing at these state configurations, and this leads to an explosive price-inflation spiral. In contrast, extended perturbation properly accounts for this upper bound, and this explains why the approximation remains stable even at these critical state configurations.

In an empirical application on the New Keynesian model, we finally use the extended perturbation approximation to re-examine whether nominal wages are more downwardly than upwardly rigid. This is an important friction as it may explain why most central banks have a positive inflation target (Kim and Ruge-Murcia (2009)) and why nominal wages were largely unaffected by the recent financial crisis in the U.S. and several European economies despite higher unemployment rates (see for instance Schmitt-Grohe and Uribe (2013) and Daly and Hobijn (2014)). We model downward nominal wage rigidity (DNWR) by asymmetric adjustment costs, which make it more costly for households to reduce than increase nominal wages. However, the asymmetry parameter in the New Keynesian model is often extremely large, and the model is therefore unlikely to be well-approximated by a standard second- or third-order perturbation solution, which in turn may

affect model inference and the resulting policy implications. For instance, Kim and Ruge-Murcia (2009) estimate the asymmetry parameter to $3,844$, whereas Abbritti and Fahr (2013) consider an even larger value of $24,100$. Re-estimating the model in Kim and Ruge-Murcia (2009) by simulated method of moments on an updated dataset, we find that standard perturbation at second and third order implies sizable DNWR, in line with previous findings in the literature. However, we somewhat surprisingly do not find any evidence of DNWR when using our more accurate extended perturbation approximation at third order, suggesting that some of the previous findings in the literature may suffer from non-neglectable approximation errors. The estimates from extended perturbation therefore imply that the optimal inflation rate is basically zero in our New Keynesian model, both under the Ramsey policy and under strict inflation targeting.

The remaining part of this paper is structured as follows. Section 2 presents the extended perturbation method, and Section 3 explores the accuracy of this approximation for a standard New Keynesian model. An efficient implementation of extended perturbation is discussed in Section 4, and Section 5 presents our empirical application. Section 6 concludes. Additional details are provided in an online appendix, and an accompanying MATLAB package implements the extended perturbation approximation.

2 The Extended Perturbation Method

We start by presenting the considered class of DSGE models in Section 2.1 and the extended perturbation method in Section 2.2. The stability of this approximation is then analyzed in Section 2.3. Given that stability can not be guaranteed when using extended perturbation beyond second order, we finally present a numerical test for stability in Section 2.4.

2.1 DSGE Models

We consider the broad class of DSGE models which can be expressed as

$$E_t \left[\mathbf{f} \left(\mathbf{x}_t, \mathbf{x}_{t+1}, \mathbf{y}_t, \mathbf{y}_{t+1} \right) \right] = \mathbf{0}, \tag{1}$$

where E_t denotes the conditional expectation given information available in period t. The state vector $\mathbf{x}_t$ with dimension $n_x \times 1$ belongs to the set $\mathcal{X}_x$, denoting Borel subsets of $\mathbb{R}^{n_x}$. The control variables are stored in $\mathbf{y}_t$ with dimension $n_y \times 1$ and $\mathbf{y}_t \in \mathcal{X}_y$, where $\mathcal{X}_y$ refers to Borel subsets of $\mathbb{R}^{n_y}$. We further let $n_x + n_y = n$. The function $\mathbf{f}$ maps elements from $\mathcal{X}_x \times \mathcal{X}_x \times \mathcal{X}_y \times \mathcal{X}_y$ into $\mathbb{R}^n$, and we assume that this mapping is at least m times differentiable, where m will be used below to indicate the approximation order of the model.

We further let $\mathbf{x}_t \equiv \begin{bmatrix} \mathbf{x}_{1,t}' & \mathbf{x}_{2,t}' \end{bmatrix}'$, where $\mathbf{x}_{1,t}$ contains the endogenous state variables and $\mathbf{x}_{2,t}$ denotes the exogenous states. The dimensions of these vectors are $n_{x_1} \times 1$ and $n_{x_2} \times 1$, respectively, with $n_{x_1} + n_{x_2} = n_x$. The dynamics of $\mathbf{x}_{2,t}$ is given by

$$\mathbf{x}_{2,t+1} = \mathbf{\Gamma}\left(\mathbf{x}_{2,t}\right) + \sigma \bar{\boldsymbol{\eta}} \boldsymbol{\epsilon}_{t+1}, \tag{2}$$

where the function $\mathbf{\Gamma}$ maps elements from $\mathcal{X}_{x_2}$ into $\mathcal{X}_{x_2}$ and is required to be at least m times differentiable. The innovations $\boldsymbol{\epsilon}_{t+1} \in \mathcal{X}_\epsilon$ has dimension $n_\epsilon \times 1$ and are assumed to be independent and identically distributed with zero mean and a unit covariance matrix, i.e. $\boldsymbol{\epsilon}_{t+1} \sim \mathcal{IID}\left(\mathbf{0}, \mathbf{I}\right)$. We also require that each element of $\boldsymbol{\epsilon}_{t+1}$ has a finite mth moment to compute the standard perturbation approximation up to mth order. The function $\mathbf{\Gamma}$ must be specified such that it generates a stable process for $\mathbf{x}_{2,t}$.[1] In linear systems, this corresponds to requiring that all eigenvalues of the Jacobian $\partial \mathbf{\Gamma} / \partial \mathbf{x}_{2,t}'$ lie inside the unit circle. For non-linear systems, $\mathbf{\Gamma}$ must satisfy the general stability condition for nonlinear first-order Markov processes provided in Section 2.3.

As in much of the perturbation literature, we focus on models with a unique solution. The exact solution may then be expressed as (see Schmitt-Grohé and Uribe (2004))

$$\mathbf{y}_t = \mathbf{g}\left(\mathbf{x}_t, \sigma\right) \tag{3}$$

$$\mathbf{x}_{t+1} = \mathbf{h}\left(\mathbf{x}_t, \sigma\right) + \sigma \boldsymbol{\eta} \boldsymbol{\epsilon}_{t+1} \tag{4}$$

[1] This implies that trends may only be included in the class of DSGE models considered if a given model after re-scaling has an equivalent representation without trending variables. A similar requirement is needed to apply the standard perturbation method. The procedure of re-scaling a DSGE model with trends is carefully described in King and Rebelo (1999).

$$\boldsymbol{\eta} \equiv \begin{bmatrix} \mathbf{0}_{n_{x_1} \times n_\epsilon} \\ \bar{\boldsymbol{\eta}} \end{bmatrix}.$$

The assumption that innovations enter linearly in (2) and (4) is without loss of generality, because the state vector may be extended to account for non-linearities between $\mathbf{x}_t$ and $\boldsymbol{\epsilon}_{t+1}$, as shown by Andreasen (2012b). The perturbation parameter $\sigma \geq 0$ scales the square root of the covariance matrix for the innovations $\boldsymbol{\eta}$ with dimension $n_x \times n_\epsilon$ and enables us to capture effects of uncertainty in the policy functions. In particular, when $\sigma = 0$ we get a model under perfect foresight, i.e.

$$\begin{aligned} \mathbf{g}^{PF}(\mathbf{x}_t) &\equiv \mathbf{g}(\mathbf{x}_t, \sigma = 0) \\ \mathbf{h}^{PF}(\mathbf{x}_t) &\equiv \mathbf{h}(\mathbf{x}_t, \sigma = 0), \end{aligned} \tag{5}$$

whereas the model with uncertainty is obtained by letting $\sigma = 1$. Unfortunately, the policy functions $\mathbf{g}$ and $\mathbf{h}$ in (3) and (4) are generally unknown and must be approximated.

2.2 The Extended Perturbation Method

Our paper builds on the observation that the policy functions can be decomposed into

$$\begin{aligned} \mathbf{g}(\mathbf{x}_t, \sigma) &\equiv \mathbf{g}^{PF}(\mathbf{x}_t) + \mathbf{g}^{stoch}(\mathbf{x}_t, \sigma) \\ \mathbf{h}(\mathbf{x}_t, \sigma) &\equiv \mathbf{h}^{PF}(\mathbf{x}_t) + \mathbf{h}^{stoch}(\mathbf{x}_t, \sigma), \end{aligned} \tag{6}$$

where $\mathbf{g}^{stoch}$ and $\mathbf{h}^{stoch}$ capture effects of uncertainty when the perfect foresight component is removed from the policy function. We also refer to $\mathbf{g}^{stoch}$ and $\mathbf{h}^{stoch}$ as the stochastic part of the policy function, as indicated by the superscript. Using (5) we clearly have that the stochastic part of the policy function is zero under perfect foresight, i.e. $\mathbf{g}^{stoch}(\mathbf{x}_t, \sigma = 0) = \mathbf{0}$ and $\mathbf{h}^{stoch}(\mathbf{x}_t, \sigma = 0) = \mathbf{0}$ for all values of $\mathbf{x}_t$. This implies that all derivatives of $\mathbf{g}$ and $\mathbf{g}^{PF}$ solely with respect to the state variables are identical at $\sigma = 0$, and similarly for $\mathbf{h}$ and $\mathbf{h}^{PF}$. That is,

$$\begin{aligned} \mathbf{g}(\mathbf{x}_t, \sigma = 0)_{\mathbf{x}^m} &= \mathbf{g}^{PF}(\mathbf{x}_t)_{\mathbf{x}^m} \quad \text{for all } \mathbf{x}_t \in \mathcal{X}_x \\ \mathbf{h}(\mathbf{x}_t, \sigma = 0)_{\mathbf{x}^m} &= \mathbf{h}^{PF}(\mathbf{x}_t)_{\mathbf{x}^m} \quad \text{for all } \mathbf{x}_t \in \mathcal{X}_x \end{aligned} \tag{7}$$

for $m = \{0, 1, 2, ...\}$, where subscripts refer to partial derivatives taken m times with respect to $\mathbf{x}_t$. We also note that all derivatives involving the perturbation parameter σ are identical for $\mathbf{g}$ and $\mathbf{g}^{stoch}$ because σ does not appear in $\mathbf{g}^{PF}$, and similarly for $\mathbf{h}$ and $\mathbf{h}^{stoch}$. That is,

$$\begin{aligned} \mathbf{g}\left(\mathbf{x}_t, \sigma\right)_{\mathbf{x}^m \sigma^j} &= \mathbf{g}^{stoch}\left(\mathbf{x}_t, \sigma\right)_{\mathbf{x}^m \sigma^j} \quad \text{for all } \mathbf{x}_t \in \mathcal{X}_x, \sigma \in \mathbb{R}_+ \\ \mathbf{h}\left(\mathbf{x}_t, \sigma\right)_{\mathbf{x}^m \sigma^j} &= \mathbf{h}^{stoch}\left(\mathbf{x}_t, \sigma\right)_{\mathbf{x}^m \sigma^j} \quad \text{for all } \mathbf{x}_t \in \mathcal{X}_x, \sigma \in \mathbb{R}_+ \end{aligned} \tag{8}$$

for $m = \{0, 1, 2, ...\}$ and $j = \{1, 2, ...\}$, where subscripts refer to partial derivatives taken m times with respect to $\mathbf{x}_t$ and j times with respect to σ. Thus, our observations in (7) and (8) imply that the standard perturbation method can be used to compute $\mathbf{g}^{stoch}\left(\mathbf{x}_t, \sigma\right)_{\mathbf{x}^m \sigma^j}$ and $\mathbf{h}^{stoch}\left(\mathbf{x}_t, \sigma\right)_{\mathbf{x}^m \sigma^j}$ at the steady state, i.e. at $\mathbf{x}_{ss} = \mathbf{x}_{t+1} = \mathbf{x}_t$ and $\sigma = 0$.

Inserting the decomposition in (6) into (3) and (4), the exact solution may be expressed as

$$\begin{aligned} \mathbf{y}_t &= \mathbf{g}^{PF}\left(\mathbf{x}_t\right) + \mathbf{g}^{stoch}\left(\mathbf{x}_t, \sigma\right) \\ \mathbf{x}_{t+1} &= \mathbf{h}^{PF}\left(\mathbf{x}_t\right) + \mathbf{h}^{stoch}\left(\mathbf{x}_t, \sigma\right) + \sigma \boldsymbol{\eta} \boldsymbol{\varepsilon}_{t+1}. \end{aligned} \tag{9}$$

Following the work of Guu and Judd (1997), the perturbation method is usually applied to approximate both $\left(\mathbf{g}^{stoch}, \mathbf{h}^{stoch}\right)$ *and* $\left(\mathbf{g}^{PF}, \mathbf{h}^{PF}\right)$ at the steady state. However, a finite Taylor series expansion of $\mathbf{g}^{PF}$ and $\mathbf{h}^{PF}$ may generate unnecessary approximation errors, given that $\mathbf{g}^{PF}$ and $\mathbf{h}^{PF}$ can be approximated to arbitrary precision by the Extended Path. We therefore suggest to compute the perfect foresight components $\mathbf{g}^{PF}$ and $\mathbf{h}^{PF}$ by the Extended Path, whereas the stochastic part of the policy function, i.e. $\mathbf{g}^{stoch}$ and $\mathbf{h}^{stoch}$, continues to be approximated by the standard perturbation method at the steady state. We name this combined solution procedure the extended perturbation method, which improves accuracy and stability of standard perturbation by removing approximation errors in the perfect foresight component of the policy function.

The approximation order in the extended perturbation method is determined by the order of the Taylor series expansion used to approximate $\mathbf{g}^{stoch}$ and $\mathbf{h}^{stoch}$. A first-order approximation

simply reproduces the perfect foresight solution, whereas the second-order approximation is

$$\begin{aligned} \mathbf{y}_t &= \mathbf{g}^{PF}(\mathbf{x}_t) + \frac{1}{2}\mathbf{g}_{\sigma\sigma}\sigma^2 \\ \mathbf{x}_{t+1} &= \mathbf{h}^{PF}(\mathbf{x}_t) + \frac{1}{2}\mathbf{h}_{\sigma\sigma}\sigma^2 + \sigma\boldsymbol{\eta}\boldsymbol{\varepsilon}_{t+1}. \end{aligned} \tag{10}$$

The third order approximation reads

$$\begin{aligned} \mathbf{y}_t &= \mathbf{g}^{PF}(\mathbf{x}_t) + \frac{1}{2}\mathbf{g}_{\sigma\sigma}\sigma^2 + \frac{3}{6}\mathbf{g}_{\sigma\sigma\mathbf{x}}\sigma^2(\mathbf{x}_t - \mathbf{x}_{ss}) + \frac{1}{6}\mathbf{g}_{\sigma\sigma\sigma}\sigma^3 \\ \mathbf{x}_{t+1} &= \mathbf{h}^{PF}(\mathbf{x}_t) + \frac{1}{2}\mathbf{h}_{\sigma\sigma}\sigma^2 + \frac{3}{6}\mathbf{h}_{\sigma\sigma\mathbf{x}}\sigma^2(\mathbf{x}_t - \mathbf{x}_{ss}) + \frac{1}{6}\mathbf{h}_{\sigma\sigma\sigma}\sigma^3 + \sigma\boldsymbol{\eta}\boldsymbol{\varepsilon}_{t+1}. \end{aligned} \tag{11}$$

In (10) and (11) derivatives of $\mathbf{g}^{stoch}$ and $\mathbf{h}^{stoch}$ known to be zero are omitted for simplicity (see Schmitt-Grohé and Uribe (2004) and Ruge-Murcia (2012)). Thus, it is straightforward to form the mth order approximation by the extended perturbation method. The required steps are:

Step 1: Run the standard perturbation method to obtain all required derivatives of $\mathbf{g}^{stoch}(\mathbf{x}_t, \sigma)$ and $\mathbf{h}^{stoch}(\mathbf{x}_t, \sigma)$ at the steady state to order m. Use these derivatives to construct the perturbation approximations of $\mathbf{g}^{stoch}(\mathbf{x}_t, \sigma)$ and $\mathbf{h}^{stoch}(\mathbf{x}_t, \sigma)$, denoted $\hat{\mathbf{g}}^{stoch}(\mathbf{x}_t, \sigma)$ and $\hat{\mathbf{h}}^{stoch}(\mathbf{x}_t, \sigma)$.

Step 2: In any time period, use the Extended Path to compute $\mathbf{g}^{PF}(\mathbf{x}_t)$ and $\mathbf{h}^{PF}(\mathbf{x}_t)$ and approximate $\mathbf{g}^{stoch}(\mathbf{x}_t, \sigma)$ and $\mathbf{h}^{stoch}(\mathbf{x}_t, \sigma)$ by $\hat{\mathbf{g}}^{stoch}(\mathbf{x}_t, \sigma)$ and $\hat{\mathbf{h}}^{stoch}(\mathbf{x}_t, \sigma)$, respectively.

2.3 Stability of the Extended Perturbation Approximation

We next analyze the stability properties of the process for $\mathbf{x}_t$ as implied extended perturbation.[2] Here, we apply the stability condition in Pötscher and Prucha (1997) for the first-order nonlinear Markov system in (4). To present this condition, iterate (4) forward by k time periods to obtain

$$\mathbf{x}_{t+k} = \mathbf{h}^{(k)}(\mathbf{x}_t, \boldsymbol{\epsilon}_{t+1}, \boldsymbol{\epsilon}_{t+2}, ...\boldsymbol{\epsilon}_{t+k-1}, \sigma) + \sigma\boldsymbol{\eta}\boldsymbol{\epsilon}_{t+k},$$

where $\mathbf{h}^{(2)}(\mathbf{x}_t, \boldsymbol{\epsilon}_{t+1}, \sigma) \equiv \mathbf{h}\left(\mathbf{h}(\mathbf{x}_t, \sigma) + \sigma\boldsymbol{\eta}\boldsymbol{\epsilon}_{t+1}, \sigma\right)$ and so forth. Pötscher and Prucha (1997) show that the system in (4) is stable if $\mathbf{h}^{(k)}$ is contracting, which is a much weaker condition than requiring

[2] Given that the control variables are functions of the states, the stability properties of $\mathbf{y}_t$ follow from those of $\mathbf{x}_t$.

$\mathbf{h}(\mathbf{x}_t, \sigma)$ to be contracting. Two sufficient conditions ensure that the contraction property holds for $\mathbf{h}^{(k)}$. The first states that there must exist an integer $k \geq 1$ at which

$$\sup \left\{ \left| \text{stac}_{j=1}^{n_x} \left[\mathbf{i}_j' \frac{\partial \mathbf{h}^{(k)}}{\partial \mathbf{x}'} \left(\mathbf{x}^j, \left\{ \boldsymbol{\epsilon}_d^j \right\}_{d=1}^{k-1}, \sigma \right) \right] \right| \right\} < 1, \tag{12}$$

given $\mathbf{x}^j \in \mathcal{X}_x$ and $\boldsymbol{\epsilon}^j \in \mathcal{X}_\epsilon$. Here, $\frac{\partial \mathbf{h}^{(k)}}{\partial \mathbf{x}'} \left(\mathbf{x}^j, \left\{ \boldsymbol{\epsilon}_d^j \right\}_{d=1}^{k-1}, \sigma \right)$ is an $n_x \times n_x$ Jacobian matrix evaluated at $\left(\mathbf{x}^j, \left\{ \boldsymbol{\epsilon}_d^j \right\}_{d=1}^{k-1} \right)$, and $|\mathbf{A}|$ denotes the norm given by the square root of the largest eigenvalue of the matrix product $\mathbf{A}'\mathbf{A}$. The vector $\mathbf{i}_j$ is the j'th column in the $n_x \times n_x$ identity matrix, and the stac-operator creates a matrix using the rows shown as arguments to the operator.[3] Hence, the condition in (12) states that for a sufficiently large integer k, the largest norm of $\partial \mathbf{h}^{(k)} / \partial \mathbf{x}'$ must be strictly smaller than one for *all* values of $\mathbf{x}_t$ and $\boldsymbol{\epsilon}_t$ in their feasible domains. The second condition for $\mathbf{h}^{(k)}$ to display the contraction property is much weaker than (12) and given by

$$\sup \left\{ \left| \frac{\partial \mathbf{h}^{(k)}}{\partial \boldsymbol{\epsilon}_l'} \left(\mathbf{x}, \{\boldsymbol{\epsilon}_d\}_{d=1}^{k-1}, \sigma \right) \right| \right\} < \infty, \tag{13}$$

where $\mathbf{x} \in \mathcal{X}_x$ and $\boldsymbol{\epsilon}_d \in \mathcal{X}_\epsilon$ for $l = 1, 2, ..., k-1$. It is clear that this second condition holds for basically all smooth approximations to DSGE models if $\mathbf{x}_t$ is finite. We therefore focus on (12) in our subsequent discussion and leave (13) as a technical regularity condition.

Before analyzing the extended perturbation approximation, it is useful to study the stability properties of the perfect foresight solution. As emphasized by Boucekkine (1995), the perfect foresight solution can only be obtained for DSGE models that are stable under perfect foresight.[4] This stability requirement means that the state process under perfect foresight $\mathbf{x}_t^{PF}$ is stable, where $\mathbf{x}_t^{PF}$ evolves as $\mathbf{x}_{t+1}^{PF} = \mathbf{h}^{PF}\left(\mathbf{x}_t^{PF}\right) + \sigma \boldsymbol{\eta} \boldsymbol{\epsilon}_{t+1}$. In other words, $\mathbf{h}^{PF}$ satisfies condition (12) and explosive sample paths for $\mathbf{x}_t^{PF}$ do not appear.

We next analyze the stability of extended perturbation when gradually increasing the approximation order, i.e. the Taylor expansion of $\mathbf{h}^{stoch}$. For this analysis, it is useful to write the extended perturbation approximation as $\mathbf{x}_{t+1} = \mathbf{h}^{ExPer}(\mathbf{x}_t, \sigma) + \sigma \boldsymbol{\eta} \boldsymbol{\varepsilon}_{t+1}$, where $\mathbf{h}^{ExPer}(\mathbf{x}_t, \sigma) \equiv$

[3] For instance, let $\mathbf{a}_j$ denote the j'th row of an $m \times n$ matrix $\mathbf{A}$, then $\text{stac}_{j=1}^{m} \mathbf{a}_j = \mathbf{A}$. The stac-operator is used in (12) to allow rows in $\partial \mathbf{h}^{(k)} / \partial \mathbf{x}'$ to be evaluated at different points, as indicated by the superindex j on the arguments at which $\partial \mathbf{h}^{(k)} / \partial \mathbf{x}'$ is evaluated.

[4] This assumption may be tested using the procedure in Boucekkine (1995).

$\mathbf{h}^{PF}(\mathbf{x}_t) + \hat{\mathbf{h}}^{stoch}(\mathbf{x}_t, \sigma)$. In a first-order approximation, there is no correction for uncertainty because $\hat{\mathbf{h}}^{stoch} = \mathbf{0}$, meaning that extended perturbation reduces to the stable perfect foresight solution.

In a second-order approximation, there is a constant correction for uncertainty as $\hat{\mathbf{h}}^{stoch} = \frac{1}{2}\mathbf{h}_{ss}\sigma^2$. This means that partial derivatives of $\mathbf{h}^{ExPer}$ with respect to the state variables are equal to those of $\mathbf{h}^{PF}$ for all values of $\mathbf{x}_t$, implying that the stability condition (12) also holds for $\mathbf{h}^{ExPer}$. Accordingly, the extended perturbation method at second order guarantees a stable approximation because the uncertainty correction only re-centers the stable perfect foresight solution.

In a third-order approximation, the uncertainty correction is a linear function of the state variables as seen in (11). This implies that partial derivatives of $\mathbf{h}^{ExPer}$ differ from those of $\mathbf{h}^{PF}$ and the stability condition (12) can not be guaranteed to hold for $\mathbf{h}^{ExPer}$, although it is satisfied for $\mathbf{h}^{PF}$. In other words, the process for $\mathbf{x}_t$ does not necessarily inherit stability from the perfect foresight solution, because $\mathbf{h}_{\sigma\sigma\mathbf{x}}$ may generate instability if the linear approximation of $\mathbf{h}^{stoch}$ is insufficiently accurate. Given that the uncertainty correction typically is small in most DSGE models, we expect that most approximations by extended perturbation will be stable.

Going beyond third order, the stochastic component of the policy function is approximated more accurately and this reduces the risk of getting unstable state dynamics with the extended perturbation method. However, as at third order, we can not guarantee a stable approximation, because partial derivatives of $\hat{\mathbf{h}}^{stoch}$ may violate the stability condition in (12) for $\mathbf{h}^{ExPer}$ although satisfied for $\mathbf{h}^{PF}$.

2.4 Testing for Stability

Given that extended perturbation does not necessarily provide a stable approximation, it seems useful to have a test to determine if a given approximation is stable or not. The test we propose applies to any approximation of DSGE models within the considered class and builds on two simplifying assumptions to get an operational version of the stability condition in (12). We first propose to only evaluate (12) on a sparse grid containing extreme state values since unstable dynamics are most likely to appear at such points. To construct the grid, let $\mathcal{S}_i = \{l_i^x, u_i^x\}$ for $i = 1, 2, ..., n_x$ contain the lower bound l_i^x and the upper bound u_i^x of the ith state variable. The

values of $\{l_i^x, u_i^x\}_{i=1}^{n_x}$ should cover the region where the approximation is used.[5] We then form the Cartesian set $\mathcal{S}_x \equiv \mathcal{S}_1 \times \mathcal{S}_2 \times ... \times \mathcal{S}_{n_x}$ which has 2^{n_x} elements. Our second simplifying assumption is only to consider the stability condition in (12) when the rows in $\partial \mathbf{h}^{(k)}/\partial \mathbf{x}'$ are evaluated at the same point.[6]

Given these simplifying assumptions, the stability condition in (12) reduces to the testable requirement that $\mathbf{h}^{(k)}$ is contracting if there exists an integer $k \geq 1$ such that

$$\max \left\{ \left| \frac{\partial \mathbf{h}^{(k)}}{\partial \mathbf{x}'} \left(\mathbf{x}, \left\{ \boldsymbol{\epsilon}_d^{(v)} \right\}_{d=1}^{k-1}, \sigma \right) \right|, \text{for all } \mathbf{x} \in \mathcal{S}_x \text{ and } v = 1, 2, ..., \mathcal{M} \right\} < 1. \tag{14}$$

Here, each point in $\mathcal{S}_x$ is evaluated using $\mathcal{M}$ sample paths of the innovations $\left\{ \boldsymbol{\epsilon}_d^{(v)} \right\}_{d=1}^{k-1}$ to avoid that a non-stable system satisfies the contraction condition just because of a "fortunate" sample path for the innovations. The test may be carried out for different values of k and $\mathcal{M}$. Some guidance on a reasonable value of k may be obtained by implementing the test on a stable linear solution.[7] We generally recommend using a fairly large value of k, say 100 or 500, because it is easier for $\mathbf{h}(\mathbf{x}_t, \sigma)$ to display the contraction property when iterated many periods forward in time. It should finally be emphasized that this stability test is not limited to the extended perturbation approximation, but may also be used for other approximations, including standard perturbation as shown in Section 3.

Another method commonly used to detect unstable approximations is to simulate multiple sample paths and see if any of these simulations explode. Compared to this brute force approach, our stability test is computationally less demanding and, more importantly, allows the researcher to locate critical state configurations, where the approximation might explode. As we will show below in Section 3, such information is valuable because it may allow the researcher to understand *why* a given approximation is unstable.

[5] Guidance on how to set these bounds may be obtained from unconditional moments or extreme values in a simulated sample using the extended perturbation approximation.

[6] At the expense of increasing the computational cost of the test, it is obvious that a finer grid for the state variables may be considered and that rows in $\partial \mathbf{h}^{(k)}/\partial \mathbf{x}'$ could be evaluated at different points.

[7] Given that the Jabocian $\partial \mathbf{h}^{(k)}/\partial \mathbf{x}'$ is computed by numerical differentiation, the most efficient implementation of the test is to evaluate $\left| \partial \mathbf{h}^{(j_{\mathbf{x}})}/\partial \mathbf{x}' \right|$ by gradually increasing $j_{\mathbf{x}}$ and then stop for a given $\mathbf{x} \in \mathcal{S}_x$ when the condition is met, even though $j_{\mathbf{x}}$ may be less than a pre-determined value of k. If $max\left\{ \{j_{\mathbf{x}}\}_{\mathbf{x} \in \mathcal{S}_x} \right\} < k$, then the stability condition in (14) is satisfied.

3 A New Keynesian Model

We next explore the accuracy and stability of standard and extended perturbation using a New Keynesian model with price stickiness as in Calvo (1983). Two reasons motivate our choice of model. First, the New Keynesian model with Calvo pricing is one of the most popular DSGE models in the literature. Second, and perhaps somewhat surprisingly, some dimensions of this New Keynesian model are highly non-linear even for a standard calibration. The strong nonlinearities in the model also imply that standard perturbation at third order easily generate explosive sample paths, suggesting that unstable approximations are not only obtained at extreme calibrations, as found in Den Haan and De Wind (2012) for the neoclassical growth model.[8] Following the standard precedure in the literature, we adopt a log-transformation and study the performance of standard and extended perturbation at third order. We proceed by describing the New Keynesian model in Section 3.1, before studying accuracy in Section 3.2 and stability in Section 3.3.

3.1 Model Description

A representative household maximizes

$$\mathcal{U}_t = E_t \sum_{l=0}^{\infty} \beta^l \left(\frac{c_{t+l}^{1-\phi_2}}{1-\phi_2} + \phi_0 \frac{(1-h_{t+l})^{1-\phi_1}}{1-\phi_1} \right), \tag{15}$$

where c_t is consumption and h_t is labor supply. In addition to a no-Ponzi-game condition, the optimization is subject to the real budget constraint

$$c_t + b_t + i_t = h_t w_t + r_t^k k_t + \frac{R_{t-1} b_{t-1}}{\pi_t} + div_t, \tag{16}$$

where resources are allocated to consumption, one-period nominal bonds b_t, and investment i_t. Letting w_t denote the real wage and r_t^k the real price of capital k_t, the household receives i) labor income $w_t h_t$, ii) income from capital services sold to firms $r_t^k k_t$, iii) payoffs from bonds purchased in the previous period $R_{t-1} b_{t-1}/\pi_t$, and iv) dividends from firms div_t. Here, $\pi_t \equiv P_t/P_{t-1}$ is gross inflation and R_t is the gross nominal interest rate. The optimization of (15) is also subject

[8] For comparability with much of the existing literature on numerical approximation methods, our online appendix contains an accuracy and stability analysis of standard and extended perturbation on the neocloassical growth model.

to the law of motion for capital $k_{t+1} = (1-\delta)\,k_t + i_t - \frac{\kappa}{2}\left(\frac{i_t}{k_t} - \psi\right)^2 k_t$, where $\kappa \geq 0$ introduces capital adjustment costs based on i_i/k_t as in Jermann (1998). The constant ψ ensures that these adjustment costs are zero in the steady state.

We consider a perfectly competitive representative firm that produces final output using $y_{i,t}$ and the production function $y_t = \left(\int_0^1 y_{i,t}^{(\eta-1)/\eta} di\right)^{\eta/(\eta-1)}$ with $\eta > 1$. This generates the demand function $y_{i,t} = \left(\frac{P_{i,t}}{P_t}\right)^{-\eta} y_t$ for the ith input $y_{i,t}$, where $P_t = \left[\int_0^1 P_{i,t}^{1-\eta} di\right]^{1/(1-\eta)}$ denotes the aggregate price level and $P_{i,t}$ is the price of the ith good.

The intermediate goods are produced by monopolistic competitors using the production function $y_{i,t} = a_t k_{i,t}^{\theta} h_{i,t}^{1-\theta}$, where technology a_t evolves as $\log a_{t+1} = \rho_a \log a_t + \sigma_a \epsilon_{a,t+1}$ with $\epsilon_{a,t+1} \sim \mathcal{NID}(0,1)$. The ith firm sets $P_{i,t}$, $h_{i,t}$, and $k_{i,t}$ by maximizing the present value of dividends. Beyond a no-Ponzi-game condition, the firm must satisfy demand for the ith good. When setting prices, we follow Calvo (1983) and assume that only a fraction $\alpha \in [0,1)$ of firms set their prices optimally, with the remaining firms letting $P_{i,t} = P_{i,t-1}$.

Finally, monetary policy is determined by the Taylor-rule

$$\log\left(\frac{R_t}{R_{ss}}\right) = \rho_R \log\left(\frac{R_{t-1}}{R_{ss}}\right) + (1-\rho_R)\left(\kappa_\pi \log\left(\frac{\pi_t}{\pi_{ss}}\right) + \kappa_y \log\left(\frac{y_t}{y_{ss}}\right)\right), \tag{17}$$

based on a desire to close the inflation gap $\log\left(\frac{\pi_t}{\pi_{ss}}\right)$ and the output gap $\log\left(\frac{y_t}{y_{ss}}\right)$, subject to smoothing changes in the policy rate with $\rho_R \in [0,1)$.

We adopt a relative standard parametrization for a quarterly model, where households have an intertemporal elasticity of substitution of 0.5 ($\phi_2 = 2$), allocate one third of their time endowment to labor in steady state ($h_{ss} = 0.33$), and have a Frisch labor supply elasticity of 1 ($\phi_1 = 2$). Firms reset prices once a year on average ($\alpha = 0.75$) and impose an average markup of 20% ($\eta = 6$). The main objective of the central bank is to stabilize inflation ($\kappa_\pi = 1.5$, $\kappa_y = 0.125$) around $\pi_{ss} = 1.00$, subject to smoothing changes in the policy rate ($\rho_R = 0.8$). The parametrization is summarized in Table 1.

3.2 Accuracy Analysis

Our New Keynesian model can be summarized by the four control variables $\left(c_t, i_t, \pi_t, x_t^2\right)$, where x_t^2 denotes an auxiliary variable for the recursive representation of firms' first-order conditions with respect to the optimal price. These control variables are a function of the states (R_{t-1}, k_t, s_t, a_t), with s_t denoting the price dispersion index linked to the Calvo pricing. One way to display these policy functions is to condition on representative values for the first three state variables, and plot the control variables as a function of the remaining state variable, i.e. technology. This exercise reveals that some of the largest differences between the approximation methods appear for a low nominal interest rate, a low capital stock, and a high value of the price dispersion index as the model here displays strong non-linearities. To conserve space, we therefore focus on this state configuration in Figure 1, before studying accuracy on a grid covering the entire state space.

The first chart of Figure 1 shows that extended perturbation captures most of the non-linear pattern in the policy function for consumption as opposed to standard perturbation when the level of technology is low. Extended perturbation therefore displays smaller errors with low values of technology (charts to the right in Figure 1), whereas the two methods display roughly similar performance for higher levels of technology. The accuracy of the two perturbation solutions is evaluated using a highly accurate 12th-order projection approximation, considered as a stand-in for the true solution.[9] The plots for the remaining control variables also reveal that there in general is a significant gain in accuracy from using extended instead of standard perturbation, in particular for investment and the auxiliary control variable x_t^2.

< Figure 1 about here >

To analyze accuracy on the entire state space, Table 2 reports root mean squared errors (RMSEs) for the considered approximation methods on a grid with 20 points uniformly spaced along each dimension of the state variables, giving a total of $20^4 = 160,000$ points. The RMSEs are computed using $\log\left(z_t / z_t^{true}\right) = \hat{z}_t - \hat{z}_t^{true}$, where $z_t \equiv \left\{c_t, i_t, \pi_t, x_t^2\right\}$ and the true solution is given by the projection approximation. We find that standard perturbation at third order is more accurate than a log-linearized approximation but is generally outperformed by the perfect foresight solution. Adding an uncertainty correction to the perfect foresight solution further improves accuracy, and

[9] See the online appendix for further details.

extended perturbation therefore delivers the best overall approximation to the four control variables. Notable improvements in RMSEs from using extended instead of standard perturbation appear for investment (0.0088 vs. 0.0172) and the auxiliary control variable (0.0387 vs. 0.0558).

< Table 2 about here >

We also study accuracy on a simulated sample path of $20,000$ observations (with a burn-in of $1,000$ observations) using the same set of innovations for technology $\{\epsilon_{a,t}\}_{t=1}^{20,000}$ in all of the approximations. Table 3 shows that extended perturbation at third order also in this setting is more accurate than standard perturbation. To explain where some of this gain in accuracy is coming from, Table 3 also reports the RMSEs for a modified version of the standard perturbation solution, where the approximated transition function for s_t in the simulation is replaced by the exact expression, i.e.

$$s_{t+1} = (1-\alpha)^{\frac{1}{1-\eta}} \left[1 - \alpha \pi_t^{\eta-1}\right]^{\frac{\eta}{\eta-1}} + \alpha \pi_t^{\eta} s_t. \tag{18}$$

That is, the price dispersion index is computed using (18) with $\pi_t = \pi_t^{3rd}$, i.e. inflation from the third-order perturbation approximation. Under the label "Perturbation: 3^{rd} order, exact s_t" in Table 3, we find that using the exact transition function for s_t lowers the RMSEs for all control variables, because we more accurately track the non-linear evolution in s_t.[10] Extended perturbation also includes the exact transition function for s_t and additional non-linearities for the control variables (although only under perfect foresight), and this explains why extended perturbation outperforms this modified perturbation approximation. We also note that extended perturbation is more accurate than the pruned third-order perturbation approximation of Andreasen, Fernandez-Villaverde, and Rubio-Ramirez (2013) which always ensures stability. The second part of Table 3 reports quarterly means and standard deviations in the simulated samples. All methods do well in matching the means, whereas we find minor negative biases in the standard deviations compared to the projection method where extended perturbation has smaller approximation errors than standard perturbation.

< Table 3 about here >

[10] Unreported results show that using the exact transition function for all endogenous state variables in combination with the standard third-order perturbation approximation of the control variables do not deliver a further improvement in accuracy.

3.3 Stability Analysis

This section uses our stability test from Section 2.4 to study the dynamic properties of standard and extended perturbation and to understand why a given approximation may be unstable. To run the stability test for the New Keynesian model, we first construct the set $\mathcal{S}_x$ with extreme state configurations. The bounds for $\hat{a}_t$ are given by ± 3 standard deviations of technology, while bounds for the two endogenous state variables $\left(\hat{R}_{t-1}, \hat{k}_t\right)$ are set to ± 4 standard deviations in a log-linearized solution, and hence slightly wider than for technology to account for effects of non-linearities. The price dispersion index $\hat{s}_t$ is constant in a log-linearized solution without steady-state inflation, and we therefore use a simulated sample path of extended perturbation to guide our bounds of -0.005 and 0.05. Using this specification of $\mathcal{S}_x$, we find that standard perturbation at third order passes our stability test with $k = 150$ and $\mathcal{M} = 50$. We also find that the extended perturbation at third order is stable with $k = 100$ and $\mathcal{M} = 50$.

Although standard perturbation at third order displays stable dynamics for the considered specification, the approximation is fragile to even minor modifications. We illustrate this point by increasing gross inflation in the steady state π_{ss} from 1.00 to 1.0015, giving an annual steady-state inflation rate of 0.6%. The bounds for $\left(\hat{R}_{t-1}, \hat{k}_t, \hat{a}_t\right)$ in the set $\mathcal{S}_x$ are determined using the same procedure as in our benchmark specification, and we increase the upper bound of $\hat{s}_t$ to 0.10. Our stability test reveals that extended perturbation at third order remains stable, whereas a third-order standard perturbation approximiation now induces unstable dynamics.[11] This implies that the explosive behavior of standard perturbation must be due to approximation errors in the perfect foresight component of the policy function, as standard and extended perturbation rely on the same approximation to the stochastic part of the policy function. An inspection of the $2^4 = 16$ extreme state configurations in $\mathcal{S}_x$ reveals that it is only when we simultaneously have a low nominal interest rate, a low capital stock, a high price dispersion index, and a low technology level that the approximation explodes when iterated forward in time to evaluate the contraction condition.[12]

To understand why standard perturbation displays unstable dynamics with $\pi_{ss} = 1.0015$, con-

[11] This result is confirmed by simulating repeated sample paths using a standard third order perturbation approximation.

[12] At this critical state configuration, we interestingly find for extended perturbation both with $\pi_{ss} = 1.00$ and $\pi_{ss} = 1.0015$ that $\mathbf{h}$ is contracting without iterating this function forward in time. This means that the number of considered sample paths $\mathcal{M}$ in the stability test is irrelevant at this state configuration for extended perturbation.

sider Figure 2 plotting the policy function for inflation and the transition equation for $\hat{s}_t$ at this state configuration. The bottom chart to the left shows that inflation in a standard perturbation approximation increases sharply for higher values of $\hat{s}_t$. This in turn leads to even higher value of the price dispersion index in the next period $\hat{s}_{t+1}$, as seen in the middle chart. This then increases $\hat{\pi}_{t+1}$, which in turn increases $\hat{s}_{t+2}$ and so on. That is, the standard perturbation approximation generates a price-inflation spiral, which eventually leads to explosive dynamics. In contrast, inflation increases only slowly in $\hat{s}_t$ with extended perturbation, because this approximation accounts for the upper bound $(1/\alpha)^{1/(\eta-1)}$ on inflation, which is implied by the Calvo pricing. This observation follows from (18), as the term $\left[1-\alpha\pi_t^{\eta-1}\right]^{\frac{\eta}{\eta-1}}$ implies complex numbers for inflation beyond $(1/\alpha)^{1/(\eta-1)}$. Accounting for the upper bound on inflation ensures broadly the same moderate increase in $\hat{s}_{t+1}$ for higher values of $\hat{s}_t$ as in the true solution (i.e. the projection approximation) and explains why extended perturbation generates stable dynamics.[13]

A careful inspection of Figure 2 also reveals that the policy functions for $\hat{\pi}_t$ and $\hat{s}_{t+1}$ in standard perturbation at third order are nearly identical for $\pi_{ss} = 1.00$ and $\pi_{ss} = 1.0015$ when considered at a given value of $\hat{s}_t$. The same applies for extended perturbation at third order. Hence, the main effect from introducing steady-state inflation is that the distribution of $\hat{s}_t$ shifts to the right and attains an even longer right tail, as shown in the third column of Figure 2. This in turn makes it more likely that we see sufficiently high values of $\hat{s}_t$ that start a price-inflation spiral in the standard perturbation approximation and generate explosive dynamics.

< Figure 2 about here >

Thus, our analysis reveals that high values of the price dispersion index s_t play an important role in generating explosive dynamics in the New Keynesian model when using standard perturbation at third order. This also means that various modifications to the New Keynesian model that lowers the degree of price dispersion in the model should reduce the probability of explosive sample paths with standard perturbation. Omitting steady state inflation is one way to reduce s_t as shown above, but one could also adopt price-indexation for non-optimizing firms by letting $P_{i,t} = P_{i,t-1}\pi_{t-1}$ as in Christiano, Eichenbaum, and Evans (2005) or increase κ_π to consider a more aggresive central bank with respect to closing the inflation gap.

[13] We conjecture that the presence of the upper bound on inflation explains the relative high approximation order needed with the projection method to obtain a sufficiently accurate approximation.

4 An Efficient Implementation of Extended Perturbation

Having documented the gain in accuracy and stability from extended perturbation, we next address its computational costs. The first step of extended perturbation involves computing derivatives of the model at the steady state, as outlined in Section 2.2. This can be done within a few seconds for third order approximations as shown in Binning (2013), and Levintal (2016) provides efficient codes up to fifth order. A computationally more demanding aspect of extended perturbation is to obtain the perfect foresight component of the policy function by the Extended Path, as it requires solving a large fixed-point problem. Although this fixed-point problem typically is solved within a few iterations using the Newton-Raphson algorithm, the computational burden may nevertheless be substantial if the perfect foresight solution is called repeatedly, for instance when simulating a long sample path.

We address this potential concern in Appendix A, where we greatly improve the numerical efficiency of Extended Path by i) deriving good starting values using a standard perturbation approximation at third order, ii) appropriately setting its terminal condition, and iii) occasionally using the standard perturbation approximation to the perfect foresight component of the policy function if it is sufficiently accurate. The latter means that we only use the Extended Path to compute $\mathbf{g}^{PF}(\mathbf{x}_t)$ and $\mathbf{h}^{PF}(\mathbf{x}_t)$ when $\mathbf{x}_t$ is far from the steady state or if the model is very non-linear along some dimensions of the state space. Appendix A shows that the three improvements may be combined to substantially reduce the computational cost of extended perturbation. Depending on the required degree of precision, we are able to simulate $1,000$ draws from a medium-sized New Keynesian model with nine state variables in 10 to 20 seconds using MATLAB on a standard desktop. Further details on each of these improvements are provided in Appendix A.

5 Application: The Level of Downward Nominal Wage Rigidity

The previous section implies that the computational costs of extended perturbation are modest even for medium-sized DSGE models, and it is therefore possible to include the approximation in existing estimation routines for non-linear DSGE models (see Duffie and Singleton (1993), Smith (1993), Fernández-Villaverde and Rubio-Ramírez (2007), Ruge-Murcia (2012), among others). We illustrate this appealing property of extended perturbation in this section by re-estimating the

New Keynesian model in Kim and Ruge-Murcia (2009) to obtain new insights about the degree of downward nominal wage regidity (DNWR). We proceed as follows. Section 5.1 starts with a brief summary of the model in Kim and Ruge-Murcia (2009) using our notation from Section 3.1. The adopted dataset and estimation methodology are described in Section 5.2. Our estimation results are presented in Section 5.3 and their robustness is explored in Section 5.4. Based on these estimates, we finally compute the optimal inflation target in Section 5.5.

5.1 A New Keynesian Model with DNWR

Households are indexed by $n \in [0,1]$ and described by

$$\mathcal{U}_{n,t} = E_t \left[\sum_{s=0}^{\infty} \beta^s d_{t+s} \left(\frac{c_{n,t+s}^{1-\phi_2}}{1-\phi_2} - \phi_0 h_{n,t+s} \right) \right], \tag{19}$$

where d_t denotes preference shocks evolving as $\log d_{t+1} = \rho_d \log d_t + \sigma_d \epsilon_{d,t}$ with $\epsilon_{d,t} \sim \mathcal{NID}(0,1)$. In contrast to the New Keynesian model in Section 3.1, we now assume that the nth household has some differentiated job skills and that it supplies labor to a continuum of firms indexed by $i \in [0,1]$. Thus, the household has some monopolistic market power and is therefore able to set both the nominal wage level $W_{n,t}$ and $h_{n,t}$ subject to firms' labor demand given by $h_{n,t} = \left(\frac{W_{n,t}}{W_t}\right)^{-\nu} h_t^d$, where ν controls the elasticity of demand for labor. Here, $h_{n,t} \equiv \int_0^1 h_{n,i,t} di$ denotes the aggregate labor supply from household n and $h_t^d \equiv \int_0^1 h_{i,t} di$ refers to the aggregated labor demand by the firms. The households are further assumed to face adjustment costs when changing the nominal wage level $W_{n,t}$. As in Kim and Ruge-Murcia (2009), we consider the specification

$$\Phi_{n,t} = \frac{\phi}{\psi^2} \left(\exp\left\{ -\psi \left(\frac{W_{n,t}}{W_{n,t-1}} - 1 \right) \right\} + \psi \left(\frac{W_{n,t}}{W_{n,t-1}} - 1 \right) - 1 \right) \tag{20}$$

with $\phi \geq 0$. Hence, ψ controls the degree of asymmetry in the these costs, which collapses to the standard quadratic specification when $\psi \to 0$.

The ith firm produces a slightly differentiable good $y_{i,t}$ using $y_{i,t} = a_t h_{i,t}^{1-\theta}$, where the labor contribution from the households is $h_{i,t} = \left[\int_0^1 h_{n,i,t}^{(\nu-1)/\nu} dn \right]^{\frac{\nu}{\nu-1}}$. Cost minimization then implies $h_{n,i,t} = \left(\frac{W_{n,t}}{W_t}\right)^{-\nu} h_{i,t}$, where $W_t \equiv \left[\int_0^1 W_{n,t}^{-(\nu-1)} dn \right]^{-\frac{1}{\nu-1}}$. Product differentiation gives each firm some monopolistic power to set its own price $P_{i,t}$, which is done subject to standard quadratic

adjustment costs $\frac{\gamma}{2}\left(\frac{P_{i,t}}{P_{i,t-1}}-1\right)^2$ per production unit.

Finally, the monetary policy is conducted according to the Taylor-rule

$$\log\left(\frac{R_t}{R_{ss}}\right)=\rho_R\log\left(\frac{R_{t-1}}{R_{ss}}\right)+(1-\rho_R)\left(\kappa_\pi\log\left(\frac{\pi_t}{\pi_{ss}}\right)+\kappa_h\log\left(\frac{h_t}{h_{ss}}\right)\right). \tag{21}$$

5.2 Data and Estimation Methodology

We use the same five quarterly data series as in Kim and Ruge-Murcia (2009) but updated to 2015Q1. That is, we consider U.S. data from 1964Q2 to 2015Q1 ($T=204$) for i) real consumption per capita, ii) hours worked, iii) quarterly CPI inflation, iv) quarterly wage inflation, and v) the nominal interest rate. All variables are stored in $\mathbf{data}_t$ with dimension 5×1. For compatibility with Kim and Ruge-Murcia (2009), all series are log-transformed and linearly detrended prior to the estimation. As in Kim and Ruge-Murcia (2009), the considered moments are the variances, the contemporaneous covariances, and the first auto-covariances for each of the series. Hence, we let

$$\mathbf{q}_t\equiv\begin{bmatrix} vec\left(\mathbf{data}_t\mathbf{data}_t'\right) \\ diag\left(\mathbf{data}_t\mathbf{data}_{t-1}'\right)\end{bmatrix}, \tag{22}$$

where $diag\left(\cdot\right)$ denotes the diagonal elements of a matrix. Letting $\boldsymbol{\theta}$ contain the model parameters, the objective function for simulated method of moment (SMM) following Duffie and Singleton (1993) is then

$$Q_{SMM}\left(\boldsymbol{\theta}\right)=\left(\frac{1}{T}\textstyle\sum_{t=1}^{T}\mathbf{q}_t-\frac{1}{\tau T}\sum_{t=1}^{\tau T}\mathbf{q}_t\left(\boldsymbol{\theta}\right)\right)'\mathbf{W}_T\left(\frac{1}{T}\textstyle\sum_{t=1}^{T}\mathbf{q}_t-\frac{1}{\tau T}\sum_{t=1}^{\tau T}\mathbf{q}_t\left(\boldsymbol{\theta}\right)\right),$$

with the estimator given by $\hat{\boldsymbol{\theta}}_{SMM}=\arg\min Q_{SMM}\left(\boldsymbol{\theta}\right)$. Here, $\frac{1}{T}\sum_{t=1}^{T}\mathbf{q}_t$ denotes the empirical moments, and $\frac{1}{\tau T}\sum_{t=1}^{\tau T}\mathbf{q}_t\left(\boldsymbol{\theta}\right)$ are the model-implied moments computed from a simulated sample path of τT observations with $\tau=10$. We adopt the conventional 2-step implementation of SMM and use a diagonal weighting matrix $\mathbf{W}_T$ based on the variance of the sample moments in a preliminary first step, before obtaining our final estimate $\hat{\boldsymbol{\theta}}$ using the optimal weighting matrix.[14]

For comparability with Kim and Ruge-Murcia (2009) we choose the same split between esti-

[14] The weigthing matrices are in both steps computed by the Newey-West estimator using $4\left(T/100\right)^{2/9}$ lags as done in the codes accompanying Kim and Ruge-Murcia (2009).

mated and calibrated parameters in the model and adopt their calibrated values. Hence, we let $\theta = 1/3$, $\beta = 0.997$, $\eta = 11$, $\nu = 3.5$, $\phi_0 = 1.00$, and $\pi_{ss} = 1.00$.

5.3 Estimation Results

As a useful benchmark, we first consider the standard specification with symmetric nominal wage adjustment costs by letting $\psi \to 0$. Panel A in Table 8 shows the estimation results for this version of the New Keynesian model using standard perturbation at second and third order as well as extended perturbation at third order. To ensure stability of standard perturbation, we apply the pruning scheme of Kim, Kim, Schaumburg, and Sims (2008) at second order and the scheme suggested by Andreasen, Fernandez-Villaverde, and Rubio-Ramirez (2013) at third order. The structural parameters attain fairly standard values for all approximations, as we find sizable adjustment costs in prices and wages and a central bank that assigns more weight to stabilizing inflation than economic activity. We also note that the difference in the estimates across the three approximations are fairly small, indicating that this version of the New Keynesian model does not display strong non-linearities and is therefore well-approximated by a standard second-order perturbation approximation.

< Table 8 >

We next consider Panel B in Table 8, where ψ is included in the set of estimated parameters. Using standard perturbation at second order, the parameter controlling the degree of DNWR is $\psi = 3,519$ with a standard error of $2,116$. A one-sided t-test of no wage asymmetry gives a P-value of 4.82%, meaning that at the 5% significance level there is evidence of DNWR based on this approximation. Kim and Ruge-Murcia (2009) draw the same conclusion using the same approximation, although they use a shorter sample ending in 2006Q2.

The empirical support for DNWR is even stronger when using standard perturbation at third order, where $\psi = 6,386$ with a standard error of $1,873$. To quantify the importance of DNWR for the ability of the New Keynesian model to fit the data, Table 8 also reports the objective functions from our two-step SMM procedure. Only the objective functions from the first step use the same weigthing matrix and are therefore comparable across models. These objective functions reveal

that DNWR induces a small improvement in the model's ability to fit the data as $Q_{SMM}^{step1} = 0.77$ compared to $Q_{SMM}^{step1} = 2.32$ without DNWR.

The final column in Table 8 shows the results from estimating the New Keynesian model with DNWR by extended perturbation at third order. We somewhat surprisingly find that there is no support for DNWR with this more accurate approximation as $\psi = 0.000$.[15] Given that we estimate the same model on the same dataset, the different estimates of DNWR must be related to the accuracy of the three approximations. Figure 4 therefore plots the exact and the approximated value of the adjustment costs in (20) as well as their marginal costs at the estimated values from standard perturbation at second and third order. The figure shows that these approximations are simply not able to capture the strong degree of non-linearity in the adjustment cost function and hence properly include effects of DNWR in the approximated solution.[16] In contrast, extended perturbation is able to capture such strong non-linearities under perfect foresight, but may introduce sizable errors in the stochastic part of the policy function. However, the presence of large approximation errors in the stochastic part of the policy function seem very unlikely for our version of the New Keynesian model, given that the households in (19) have linear disutility of labor and therefore are risk-neutral (see Swanson (2012)). A conjecture which is supported by the very small elements in $(\mathbf{g}_{\sigma\sigma}, \mathbf{h}_{\sigma\sigma})$ and $(\mathbf{g}_{\sigma\sigma\mathbf{x}}, \mathbf{h}_{\sigma\sigma\mathbf{x}})$ from the standard perturbation approximation.

A much more likely explanation for the lack of DNWR in the estimates from extended perturbation is offered by Figure 5, which shows the detrended time series of nominal wage inflation used in the estimation. According to this time series, the U.S. economy has experienced frequent spells of both positive and negative nominal wage inflation, with 52.9% of the observations representing a fall in nominal wages. This may help to explain why we do not find sizable DNWR when estimated by extended perturbation, because strong DNWR would make it hard for our New Keynesian model to generate frequent spells of negative nominal wage inflation as observed in the data.

< Figure 5 about here >

[15] The estimates from Panel A were used as starting values for the optimization, but allowing for $\psi > 0$ did not improve the fit. We also tried repeately to set the initial value of ψ to 50 or even larger values, but the optimizer (e.g. the Nelder-Mead simplex routine) never found a better value for the object function than the reported estimates.

[16] We should emphasize that this finding does *not* imply that standard perturbation never should be apply to the cost function in (20). For instance, if ψ is lowered to 100 and the value of ϕ is unchanged compared to Table 8, then standard perturbation at second and third order actually provide a fairly accurate approximation.

5.4 Robustness Analysis

Based on Figure 5 it seems natural to explore whether the lack of DNWR when using extended perturbation is explained by the adopted de-trending procedure of nominal variables in our analysis. Hence, we next re-estimate the New Keynesian model without de-trending inflation, nominal wage inflation, and the nominal interest rate prior to the estimation as done in Section 5.3. Instead, the mean of these three variables are now included in the set of moments for SMM, where π_{ss} also is added to the estimated parameters to give the model a fair chance of matching these unconditional means. However, unreported estimation results show that our results are robust to including a nominal trend, as we also for this alternative specification do not find evidence of DNWR when using extended perturbation at third order.

Another explanation for the lack of DNWR might be that the considered moments in (22) are symmetric in their arguments, and hence may be unable to adequately capture any asymmetry in nominal wages. To explore this possibility, we next let $W_t^{gr} \equiv \Delta \log W_t$ denote nominal wage growth and extend the set of moments in (22) by $E\left[1_{\{W_t^{gr}\geq 0\}} W_t^{gr}\right]$, $E\left[1_{\{W_t^{gr}<0\}} W_t^{gr}\right]$, $E\left[1_{\{W_t^{gr}\geq 0\}} (W_t^{gr})^2\right]$, and $E\left[1_{\{W_t^{gr}<0\}} (W_t^{gr})^2\right]$. For comparability with our benchmark analysis in Section 5.3, all nominal variables are detrended prior to the estimation as described in Section 5.2. However, the estimation results once again show no evidence of DNWR as $\psi = 0.000$, despite including these four additional moments tailored to capture any nominal wage asymmetry.

5.5 The Optimal Inflation Target

Finally, we compute the optimal monetary policy by solving the Ramsey problem for the estimates reported in Table 8. That is, the interest rate is no longer given by (21) but determined by optimizing the utility function in (19) subject to the resource constraint and the first order conditions for the households and firms. The optimal inflation rate implied by the Ramsey policy is then given by the unconditional mean of inflation which we compute by simulation using a sample path of τT observations as in Section 5.3.

For standard perturbation at second order, the optimal annual inflation rate is 0.03%, which is somewhat lower than the optimal level of 0.35% found in Kim and Ruge-Murcia (2009). This difference is almost entirely explained by our high estimate of $\phi^{2nd} = 1,072.8$, as the optimal

inflation rate increases to 0.31% if let $\phi = 280.4$ as found in Kim and Ruge-Murcia (2009) using a somewhat shorter sample. For the standard perturbation at third order, the annual optimal inflation rate is basically zero (0.003%), which is not too surprising given the very high estimate of $\phi^{3rd} = 5,082.9$.[17] In the case of extended perturbation, the annual optimal inflation rate is 0.001%, which is to be expected given the lack of DNWR for these estimates.

As a supplement to the optimal inflation rate for the Ramsey policy, we also report the utility maximizing level of π_{ss} under strict inflation targeting. Conditioning on the estimated values, standard perturbation at second order implies $\pi_{ss} = 1.0021$, which corresponds to an annual inflation target of 0.84%. This inflation level is thus very close to the 0.75% per year found in Kim and Ruge-Murcia (2009) for strict inflation targeting. For the standard perturbation at third order, we find $\pi_{ss} = 1.0015$ under strict inflation targeting, which is equivalent to an annual inflation rate of 0.60%. Finally, for extended perturbation at third order, the optimal inflation rate is $\pi_{ss} = 1.0003$.

Based on these findings we conclude that the three estimates of the New Keynesian model all predict zero inflation under the Ramsey policy, whereas the policy recommendations differ under strict inflation targeting.

6 Conclusion

This paper introduces the extended perturbation method which improves the accuracy and stability of standard perturbation by using a better approximation to the perfect foresight component of the policy function. For the New Keynesian model with Calvo pricing, we show that extended perturbation achieves higher accuracy than standard perturbation. We also show that the gain in accuracy is sufficient to generate stable approximations by extended perturbation when standard perturbation explodes. Our results therefore suggest that the explosive behavior of standard perturbation reported in the literature may be related to inaccuracies in the perfect foresight component of the policy function and may be eliminated by using extended perturbation. To reduce the computational costs of implementing extended perturbation, we also introduce several improvements of the Extended Path which substantially lowers execution costs and makes extended perturbation

[17] Using $\phi = 280.4$ as found in Kim and Ruge-Murcia (2009), we get an annual optimal inflation rate of 0.90%.

feasible for estimation.

In an empirical application, we use a New Keynesian model to re-examine whether nominal wages are more downwardly than upwardly rigid. When using standard perturbation at second and third order we find sizable DNWR, but not when using our more accurate extended perturbation approximation at third order. This suggests that some of the previous findings on DNWR in the literature may suffer from non-neglectable approximation errors. Despite the different estimates of DNWR, the preferred inflation rate is zero under the Ramsey policy, whereas the policy recommendations differ under strict inflation targeting.

A Numerical Efficiency of Extended Perturbation

This appendix presents several ways to reduce the time spent computing the perfect foresight component of the policy function in extended perturbation. That is, the focus of this appendix is entirely devoted to the perfect foresight solution.

A.1 Expanding the New Keynesian Model

Given that many non-linear solution methods either perform poorly or become infeasible in large models, we first extend our model from Section 3 to study the computational complexity of extended perturbation on a fairly large model. We therefore replace the utility function in (15) by

$$\mathcal{U}_t = E_t \sum_{l=0}^{\infty} \beta^l d_{t+l} \left(\frac{(c_{t+l} - b c_{t-1+l})^{1-\phi_2}}{1-\phi_2} + \phi_0 \frac{(1-h_{t+l})^{1-\phi_1}}{1-\phi_1} \right),$$

where b introduces external habit formation and d_t are preference shocks evolving as $\log d_{t+1} = \rho_d \log d_t + \sigma_d \epsilon_{d,t}$ with $\epsilon_{d,t} \sim \mathcal{NID}(0,1)$. We also augment (17) with monetary policy shocks $\sigma_R \epsilon_{R,t}$ where $\epsilon_{R,t} \sim \mathcal{NID}(0,1)$, and introduce investment specific shocks e_t by replacing (16) with

$$c_t + b_t + i_t/e_t = h_t w_t + r_t^k k_t + \frac{R_{t-1} b_{t-1}}{\pi_t} + div_t,$$

where $\log e_{t+1} = \rho_e \log e_t + \sigma_e \epsilon_{e,t+1}$ and $\epsilon_{e,t+1} \sim \mathcal{NID}(0,1)$. Finally, trends in technology are introduced through z_t in the production function, i.e. $y_{i,t} = a_t k_{i,t}^{\theta} (z_t h_{i,t})^{1-\theta}$ where $\log z_{t+1} = \log \mu_{z,ss} + \log z_t + \sigma_z \epsilon_{z,t+1}$ and $\epsilon_{z,t+1} \sim \mathcal{NID}(0,1)$. As a result, this extended New Keynesian model has five shocks and nine state variables, making its size comparable to many of the DSGE models typically used in the literature to study business cycles (see for instance Christiano, Eichenbaum, and Evans (2005), Fernández-Villaverde and Rubio-Ramírez (2007), among others).[18]

For the simulation experiments below, we let $b = 0.3$, $\rho_d = 0.98$, $\rho_e = 0.90$, $\sigma_d = 0.015$, $\sigma_e = 0.01$, $\sigma_R = 0.0025$, $\mu_z = 1.005$, and $\pi_{ss} = 1.005$. Given the additional shocks and steady state inflation of 2% per year, we initially eliminate the price-inflation spiral in the standard third-order perturbation approximation by letting $\kappa_\pi = 2.0$ to make the central bank more aggressive to deviations in the inflation gap. With the remaining parameters given by Table 1, we obtain a calibration where standard perturbation at third order generates stable dynamics. This specification is therefore referred to as the 'stable perturbation calibration'. It is also useful to consider a setting where standard third-order perturbation explodes. We therefore lower κ_π to 1.95 in our second calibration (which is otherwise identical to the first calibration) and refer to this second specification as the 'explosive perturbation calibration'.

A.2 Efficient Starting Values for the Extended Path

It is essential to have good starting values to obtain fast convergence when solving the fixed-point problem implied by the Extended Path. These starting values are typically derived based on a first-order approximation. However, when the Extended Path is used in the extended perturbation method, higher-order derivatives of the functions **g** and **h** are already available as they are required

[18] The computational cost of running the Extended Path is largely unaffected by the number of exogenous shocks because they are concentrated out when solving the fixed-point problem, as explained in our online appendix. Hence, the execution time reported below for the perfect foresight component of the policy function should be representative of the computational costs implied by models with more than five structural shocks.

to compute the uncertainty corrections. It therefore seems natural to use these higher-order derivatives to improve the starting values from a linearized solution. To minimize the computational burden of deriving $\{E_t[\mathbf{x}_{t+i}], E_t[\mathbf{y}_{t+i-1}]\}_{i=1}^{N}$, we use the perturbation method of Andreasen and Zabczyk (2015).[19] The method is outlined in Appendix B for a third-order approximation.

We evaluate the effect of different starting values in the Extended Path by simulating a sample path of $5,000$ observations. For the stable perturbation calibration it takes $2,465$ seconds to generate this sample path when using starting values from a linearized solution, but only $1,926$ seconds when the starting values are obtained from a third-order approximation. This is equivalent to an efficiency gain of 21.9%.[20] The corresponding execution times for the explosive perturbation calibration are $2,878$ and $2,478$ seconds, respectively, and imply an efficiency gain of 13.9%.[21] Given these findings, we use starting values from standard perturbation at third order in the remaining part of this appendix.

A.3 The Terminal Condition in the Extended Path

The execution time of the Extended Path is also affected by the length of the horizon N considered before closing the approximated system with a terminal condition for the control variables $\mathbf{y}_{t+N}$. As the size of the fixed-point problem in the Extended Path grows linearly in N, it is desirable to use a relatively low value of N. Adjemian and Juillard (2010) note that N can be lowered if the standard terminal condition of $\mathbf{y}_{t+N} = \mathbf{y}_{ss}$ is replaced by $\mathbf{y}_{t+N} = E_t\left[\mathbf{y}_{t+N}^{1st}\right]$, where $\mathbf{y}_{t+N}^{1st}$ denotes the control variables at time $t+N$ in a first-order approximation. But, higher-order approximations to the conditional expectation of $\mathbf{y}_{t+N}$ are easily obtained from the process of computing efficient starting values in Section A.2, and it therefore seems natural to consider the terminal condition $\mathbf{y}_{t+N} = E_t\left[\mathbf{y}_{t+N}^{3rd}\right]$, with $\mathbf{y}_{t+N}^{3rd}$ denoting the control variables at time $t+N$ in a third-order approximation.

Table 4 analyzes the accuracy of the Extended Path with respect to the horizon N and the choice of terminal condition on a simulated sample path of $5,000$ observations. For both calibrations, all terminal conditions imply the same level of accuracy with a long horizon of $N = 250$, which serves as the benchmark for computing the RMSEs. When we gradually reduce N, the standard terminal condition of $\mathbf{y}_{t+N} = \mathbf{y}_{ss}$ is clearly less accurate compared to using the terminal condition from a linearized solution. The final column in Table 4 shows that a third-order approximation for the terminal condition is even more accurate than the linearized solution, except when $N = 50$ in the explosive perturbation calibration. Hence, we generally obtain the highest level of accuracy in the Extended Path by using a third-order approximation to compute the terminal condition, and we therefore adopt this specification in the remainder of this appendix.

< Table 4 about here >

A.4 A State-dependent Horizon in the Extended Path

So far, we have assumed that the same horizon applies to all state values in the Extended Path. But if $\mathbf{x}_t$ is close to the steady state, a relative short horizon should be sufficient for $E_t\left[\mathbf{y}_{t+N}^{3rd}\right]$. We

[19] Given a third-order perturbation approximation and $N = 200$, it takes only 0.04 and 0.40 seconds to compute the required loadings for the conditional expectations up to second and third order, respectively, in our New Keynesian model.

[20] The computations are carried out in MATLAB 2014a using an Intel(R) Core(TM) i5-4200 CPU with 2.50 GHz and a horizon of $N = 200$ in the Extended Path.

[21] The execution times are slightly higher in this second calibration, because it is time-consuming to obtain convergence in the Extended Path for state values far from the steady state where standard perturbation explodes.

exploit this observation to introduce a state-dependent horizon N^*, where the aim is to dynamically adjust the horizon to reduce the computational cost of the Extended Path. We implement this idea by the rule

$$N^*\left(D_{ss},\mathbf{x}_t\right)=\min\left\{N\in\mathbb{N}:\max\left\{\left|E_t\left[\mathbf{y}_{t+N}^{3rd}\right]\right|\right\}\leq D_{ss}\quad\text{st.}\quad N\in[N_{\min},N_{\max}]\right\},\tag{23}$$

where D_{ss} denotes the tolerated distance of $E_t\left[\mathbf{y}_{t+N}^{3rd}\right]$ from the steady state. That is, we use the shortest horizon where the largest element in $E_t\left[\mathbf{y}_{t+N}^{3rd}\right]$ is within the distance D_{ss} from the steady state, subject to $N\in[N_{\min},N_{\max}]$. This implies that N^* depends on D_{ss} and the current state $\mathbf{x}_t$ through $E_t\left[\mathbf{y}_{t+N}^{3rd}\right]$, as indicated in (23).

Table 5 evaluates the performance of N^* with $N_{\min}=20$ and $N_{\max}=200$ on a simulated sample path of $5,000$ observations. The execution time with a fixed horizon of $N=200$ corresponds to $D_{ss}=0$ and requires 385 seconds per $1,000$ draws. Introducing the state-dependent horizon with $D_{ss}=0.01$ hardly implies any loss of accuracy ($RMSE=7.91\times10^{-5}$), but reduces the execution time to just 196 seconds per $1,000$ draws due to an average horizon of just 87 time periods. For larger values of D_{ss}, the average horizon and the execution time fall even further but it also affects the accuracy of the Extended Path. Turning to the explosive perturbation calibration in the lower part of Table 5, we once again find that a state-dependent horizon lowers the execution time of the Extended Path with only a small loss in accuracy.

< Table 5 about here >

A.5 Occasionally Using the Perturbation Approximation of the Perfect Foresight Component

We have so far used the Extended Path to compute the perfect foresight component of the policy function for all state values. But a standard perturbation approximation to this component may for some state values be sufficiently accurate. To formalize this idea, let $\mathbf{y}_t^{3rd}$ denote the standard perturbation approximation at third order to the control variables at $\mathbf{x}_t$. The standard perturbation approximation of $E_t\left[\mathbf{y}_{t+1}^{3rd}\right]$ is derived in Section A.2, and $\mathbf{x}_{t+1}^{3rd}$ follows directly from approximated state equations. We then use (1) to compute the Euler-equation residuals under perfect foresight of the standard perturbation approximation in period t, i.e. $\mathbf{\Psi}_t\equiv\mathbf{f}\left(\mathbf{x}_t,\mathbf{x}_{t+1}^{3rd},\mathbf{y}_t^{3rd},E_t\left[\mathbf{y}_{t+1}^{3rd}\right]\right)$, where $\mathbf{f}$ is expressed in unit-free terms. Next, let EE denote the tolerated Euler-equation errors, and consider the approximation

$$\begin{array}{c}\mathbf{y}_t=1_{\{\max|\mathbf{\Psi}_t|\leq EE\}}\mathbf{g}^{3rd}\left(\mathbf{x}_t\right)+\left(1-1_{\{\max|\mathbf{\Psi}_t|\leq EE\}}\right)\mathbf{g}^{PF}\left(\mathbf{x}_t\right)\\ \mathbf{x}_{t+1}=1_{\{\max|\mathbf{\Psi}_t|\leq EE\}}\mathbf{h}^{3rd}\left(\mathbf{x}_t\right)+\left(1-1_{\{\max|\mathbf{\Psi}_t|\leq EE\}}\right)\mathbf{h}^{PF}\left(\mathbf{x}_t\right)+\sigma\boldsymbol{\eta}\boldsymbol{\epsilon}_{t+1}\end{array},\tag{24}$$

where $1_{\{\max|\mathbf{\Psi}_t|\leq EE\}}$ is the indicator function. Here, $\mathbf{g}^{3rd}\left(\mathbf{x}_t\right)$ denotes the standard perturbation approximation to the perfect foresight component of the policy function, and similarly for $\mathbf{h}^{3rd}\left(\mathbf{x}_t\right)$. That is, we use standard perturbation when it is sufficiently accurate, i.e. $\max|\mathbf{\Psi}_t|\leq EE$, otherwise the Extended Path is used.

The performance of (24) is shown in Table 6 for the stable perturbation calibration using a simulated sample path of $5,000$ observations. The first part of the table imposes $D_{ss}=0$ and uses a fixed horizon of $N=200$ in the Extended Path. Letting $EE=5\times10^{-5}$, the Extended Path is only used for 27% of the observations, and this allows us to generate $1,000$ draws in just 58 seconds compared to 385 seconds with $EE=0$. This sizable reduction in execution time is achieved with nearly no loss in accuracy as seen from the RMSEs of 3.28×10^{-5}. For larger values of EE, even

more observations are computed by the perturbation approximation and this further reduces the computational cost at the expense of a small loss in accuracy.[22] The remaining part of Table 6 adds a state-dependent horizon to the Extended Path and this further lowers the execution time.

< Table 6 about here >

The results for the explosive perturbation calibration in Table 7 also document a large reduction in execution costs with only a small loss in accuracy by occasionally using the perturbation approximation. With a relatively high value of EE, we only use the Extended Path to avoid explosive sample paths and otherwise rely on the standard perturbation approximation. This is illustrated in Figure 3, where we plot $\|\hat{\mathbf{x}}_t\| = \sqrt{\sum_{i=1}^{n_x} \hat{x}_{i,t}^2}$ for the part of our simulated sample where standard perturbation explodes. With a high value of EE as considered in the bottom chart, extended perturbation only relies on the Extended Path (marked by gray areas) from observation 4125 to 4250 where standard perturbation explodes, as shown by the diverting blue line. The case with a relatively low value of EE is considered in the top chart of Figure 3, where the Extended Path is used to avoid explosive dynamics and improve accuracy even when standard perturbation does not explode.

< Figure 3 and Table 7 about here >

B Conditional Expectations in DSGE Models

Consider the case where the DSGE model reports the endogenous variable r_t and we want to compute conditional expectations of this variable, i.e. $r_{1,t} \equiv E_t[r_{t+1}]$, $r_{2,t} \equiv E_t[r_{t+2}]$, $r_{3,t} \equiv E_t[r_{t+3}]$, etc.[23] The law of iterated expectations implies $r_{2,t} \equiv E_t[r_{t+2}] = E_t[E_{t+1}[r_{t+2}]] = E_t[r_{1,t+1}]$ and so on. Hence, only a formula for computing $p_t \equiv E_t[r_{t+1}]$ is needed because all other expectations can be found be iterating on this formula. We therefore consider the problem

$$p(\mathbf{x}_t) = E_t[r(\mathbf{x}_{t+1})],$$

where we omit the perturbation parameter σ, given our focus on the perfect foresight solution.[24] We then observe that

$$F(\mathbf{x}_t) \equiv E_t\left[-p(\mathbf{x}_t) + r\left(\mathbf{h}(\mathbf{x}_t) + \sigma\boldsymbol{\eta}\boldsymbol{\epsilon}_{t+1}\right)\right] = 0, \tag{25}$$

because $\mathbf{x}_{t+1} = \mathbf{h}(\mathbf{x}_t) + \sigma\boldsymbol{\eta}\boldsymbol{\epsilon}_{t+1}$. Note then that (25) must hold for all values of $\mathbf{x}_t$. This allow us to compute all derivatives of p with respect to $\mathbf{x}_t$ around the deterministic steady state, i.e. $\mathbf{x}_t = \mathbf{x}_{ss}$ and $\sigma = 0$, given derivatives of $\mathbf{h}(\mathbf{x}_t)$ and $r(\mathbf{x}_{t+1})$ around the same point. For the indices we adopt the convention that the subscript indicates the order of differentiation. I.e. a subscript 1 is for the first time we take derivatives and so on. Thus,

$$\alpha_1, \alpha_2, \alpha_3 = 1, 2, ..., n_x \qquad \gamma_1, \gamma_2, \gamma_3 = 1, 2, ..., n_x.$$

[22] When $EE = 0.01$ all observations are computed by the perturbation approximation. Its execution time is here higher than reported in Table 5, mainly due to the computational costs of obtaining $\boldsymbol{\Psi}_t$.

[23] If the variable of interest is a control variable, then the function $r(\mathbf{x}_{t+1})$ follows from the function $\mathbf{g}(\cdot)$. If the variable of interest is a state variable, then we let $r_t \equiv \mathbf{i}'\mathbf{x}_t$ to obtain moments for the i'th state variable with $i(k,1) = 1$ for $k = i$, otherwise $i(k,1) = 0$.

[24] Derivatives of the conditional expectation with respect to the perturbation parameter are derived in a technical appendix accompanying Andreasen (2012a).

To compute the first-order terms, straightforward differentiation of (25) implies

$$[p_{\mathbf{x}}]_{\alpha_1} = [r_{\mathbf{x}}]_{\gamma_1} [\mathbf{h}_{\mathbf{x}}]^{\gamma_1}_{\alpha_1},$$

or in standard matrix notation

$$\mathbf{p}_{\mathbf{x}}(1;:) = \mathbf{r}_{\mathbf{x}}(1,:)\,\mathbf{h}_{\mathbf{x}}.$$

The second-order terms are given by

$$[p_{\mathbf{xx}}]_{\alpha_1\alpha_2} = [r_{\mathbf{xx}}]_{\gamma_1\gamma_2} [\mathbf{h}_{\mathbf{x}}]^{\gamma_2}_{\alpha_2} [\mathbf{h}_{\mathbf{x}}]^{\gamma_1}_{\alpha_1} + [r_{\mathbf{x}}]_{\gamma_1} [\mathbf{h}_{\mathbf{xx}}]^{\gamma_1}_{\alpha_1\alpha_2},$$

or in the standard matrix notation

$$\mathbf{p}_{\mathbf{xx}} = \mathbf{h}'_{\mathbf{x}}\mathbf{r}_{\mathbf{xx}}\mathbf{h}_{\mathbf{x}} + \textstyle\sum_{\gamma_1=1}^{n_x} \mathbf{r}_{\mathbf{x}}(1,\gamma_1)\,\mathbf{h}_{\mathbf{xx}}(\gamma_1,:,:),$$

where $\mathbf{h}_{\mathbf{xx}}$ has dimensions $n_x \times n_x \times n_x$ and contains all second order derivatives of $\mathbf{h}(\cdot)$ with respect to $(\mathbf{x}_t, \mathbf{x}_t)$. Finally, the third-order terms are given by

$$\begin{aligned}
[p_{\mathbf{xxx}}]_{\alpha_1\alpha_2\alpha_3} &= [r_{\mathbf{xxx}}]_{\gamma_1\gamma_2\gamma_3} [\mathbf{h}_{\mathbf{x}}]^{\gamma_3}_{\alpha_3} [\mathbf{h}_{\mathbf{x}}]^{\gamma_2}_{\alpha_2} [\mathbf{h}_{\mathbf{x}}]^{\gamma_1}_{\alpha_1} \\
&\quad + [r_{\mathbf{xx}}]_{\gamma_1\gamma_2} [\mathbf{h}_{\mathbf{xx}}]^{\gamma_2}_{\alpha_2\alpha_3} [\mathbf{h}_{\mathbf{x}}]^{\gamma_1}_{\alpha_1} \\
&\quad + [r_{\mathbf{xx}}]_{\gamma_1\gamma_2} [\mathbf{h}_{\mathbf{x}}]^{\gamma_2}_{\alpha_2} [\mathbf{h}_{\mathbf{xx}}]^{\gamma_1}_{\alpha_1\alpha_3} \\
&\quad + [r_{\mathbf{xx}}]_{\gamma_1\gamma_3} [\mathbf{h}_{\mathbf{x}}]^{\gamma_3}_{\alpha_3} [\mathbf{h}_{\mathbf{xx}}]^{\gamma_1}_{\alpha_1\alpha_2} \\
&\quad + [r_{\mathbf{x}}]_{\gamma_1} [\mathbf{h}_{\mathbf{xxx}}]^{\gamma_1}_{\alpha_1\alpha_2\alpha_3},
\end{aligned}$$

or in the standard matrix notation

$$\begin{aligned}
\mathbf{p}_{\mathbf{xxx}}(\alpha_1,\alpha_2,\alpha_3) &= \textstyle\sum_{\gamma_3=1}^{n_x} \mathbf{h}_{\mathbf{x}}(:,\alpha_1)'\,\mathbf{r}_{\mathbf{xxx}}(:,:,\gamma_3)\,\mathbf{h}_{\mathbf{x}}(:,\alpha_2)\,\mathbf{h}_{\mathbf{x}}(\gamma_3,\alpha_3) \\
&\quad + \mathbf{h}_{\mathbf{x}}(:,\alpha_1)'\,\mathbf{r}_{\mathbf{xx}}\mathbf{h}_{\mathbf{xx}}(:,\alpha_2,\alpha_3) \\
&\quad + \textstyle\sum_{\gamma_1=1}^{n_x} \mathbf{r}_{\mathbf{xx}}(\gamma_1,:)\,\mathbf{h}_{\mathbf{x}}(:,\alpha_2)\,\mathbf{h}_{\mathbf{xx}}(\gamma_1,\alpha_1,\alpha_3) \\
&\quad + \textstyle\sum_{\gamma_1=1}^{n_x} \mathbf{r}_{\mathbf{xx}}(\gamma_1,:)\,\mathbf{h}_{\mathbf{x}}(:,\alpha_3)\,\mathbf{h}_{\mathbf{xx}}(\gamma_1,\alpha_1,\alpha_2) \\
&\quad + \mathbf{r}_{\mathbf{x}}(1,:)\,\mathbf{h}_{\mathbf{xxx}}(:,\alpha_1,\alpha_2,\alpha_3).
\end{aligned}$$

Here, $\mathbf{h}_{\mathbf{xxx}}$ has dimensions $n_x \times n_x \times n_x \times n_x$ and contains all third order derivatives of $\mathbf{h}(\cdot)$ with respect to $(\mathbf{x}_t, \mathbf{x}_t, \mathbf{x}_t)$. Similarly, $\mathbf{r}_{\mathbf{xxx}}$ and $\mathbf{p}_{\mathbf{xxx}}$ have dimensions $n_x \times n_x \times n_x$ and contain all third order derivatives of the r- and p-functions, respectively.

References

Abbritti, M., and S. Fahr (2013): "Downward wage rigidity and business cycle asymmetries," *Journal of monetary economics*, 60, 871–886.

Adjemian, S., and M. Juillard (2010): "Dealing with ZLB in DSGE models: An application to the Japanese Economy," *ESRI Discussion Paper No. 258*.

An, S., and F. Schorfheide (2007): "Bayesian Analysis of DSGE Models," *Econometric Review*, 26(2-4), 113–172.

Andreasen, M. M. (2012a): "An Estimated DSGE Model: Explaining Variation in Nominal Term Premia, Real Term Premia, and Inflation Risk Premia," *European Economic Review*, 56, 1656–1674.

——— (2012b): "On the Effects of Rare Disasters and Uncertainty Shocks for Risk Premia in Non-Linear DSGE Models," *Review of Economic Dynamics*, 15, 295–316.

Andreasen, M. M., J. Fernandez-Villaverde, and J. F. Rubio-Ramirez (2013): "The Pruned State Space System for Non-Linear DSGE Models: Theory and Empirical Applications to Estimation," *NBER Working Paper*.

Andreasen, M. M., and P. Zabczyk (2015): "Efficient Bond Price Approximations in Non-Linear Equilibrium-Based Term Structure Models," *Studies in Nonlinear Dynamics and Econometrics*, 19(1), 1–34.

Binning, A. (2013): "Solving second and third-order approximations to DSGE models: A recursive Sylvester equation solution," *Norges Bank, Working Paper 18*.

Boucekkine, R. (1995): "An alternative methodology for solving nonlinear forward-looking models," *Journal of Economic Dynamics & Control*, 19, 711–734.

Calvo, G. A. (1983): "Staggered Prices in a Utility-Maximizing Framework," *Journal of Monetary Economics*, 12, 383–398.

Christiano, L. J., M. Eichenbaum, and C. L. Evans (2005): "Nominal Rigidities and the Dynamic Effects of a Shock to Monetary Policy," *Journal of Political Economy*, 113, 1–45.

Daly, M. C., and B. Hobijn (2014): "Downward Nominal Wage Rigidities Bend the Phillips Curve," *Journal of Money, Credit and Banking*, Supplement to 46(2), 51–93.

Den Haan, W. J., and J. De Wind (2012): "Nonlinear and stable perturbation-based approximations," *Journal of Economic Dynamics & Control*, 36, 1477–1497.

Duffie, D., and K. J. Singleton (1993): "Simulated Moments Estimation of Markov Models of Asset Prices," *Econometrica*, 61(4), 929–952.

Fair, R. C., and J. B. Taylor (1983): "Solution and Maximum Likelihood Estimation of Dynamic Nonlinear Rational Expectations Models," *Econometrica*, 51, 1169–1185.

Fernández-Villaverde, J., P. Guerrón-Quintana, J. F. Rubio-Ramírez, and M. Uribe (2011): "Risk Matters: The Real Effects of Volatility Shocks," *American Economic Review*, 101, 2530–2561.

Fernández-Villaverde, J., and J. F. Rubio-Ramírez (2007): "Estimating Macroeconomic Models: A Likelihood Approach," *Review of Economic Studies*, 74, 1–46.

Guu, S.-M., and K. L. Judd (1997): "Asymptotic methods for aggregate growth models," *Journal of Economic Dynamics & Control*, 21, 1025–1042.

Jermann, U. J. (1998): "Asset Pricing in Production Economics," *Journal of Monetary Economics*, 41, 257–275.

Kim, J., S. Kim, E. Schaumburg, and C. A. Sims (2008): "Calculating and using second-order accurate solutions of discrete time dynamic equilibrium models," *Journal of Economic Dynamics & Control*, 32, 3397–3414.

Kim, J., and F. J. Ruge-Murcia (2009): "How much inflation is necessary to grease the wheels?," *Journal of Monetary Economics*.

King, R. G., and S. T. Rebelo (1999): "Resuscitating Real Business Cycles," *Handbook of Macroeconomics*, 1, 927–1007.

Levintal, O. (2016): "Fifth-Order Perturbation Solution to DSGE Models," *Working Paper, Interdisciplinary Center Herzliya, School of Economics*.

Lombardo, G., and H. Uhlig (2014): "A Theory of Pruning," *European Central Bank, Working Paper Series number 1696*.

Pötscher, B. M., and I. Prucha (1997): *Dynamic Nonlinear Econometric Models: Asymptotic Theory*. Springer.

Rudebusch, G. D., and E. T. Swanson (2012): "The Bond Premium in a DSGE Model with Long-Run Real and Nominal Risks," *American Economic Journal: Macroeconomics*, 4(1), 105–143.

Ruge-Murcia, F. (2012): "Estimating nonlinear DSGE models by the simulated method of moments: With an application to business cycles," *Journal of Economics Dynamic and Control*, 35, 914–938.

Schmitt-Grohe, S., and M. Uribe (2013): "Downward Nominal Wage Rigidity and the Case for Temporary Inflation in the Eurozone," *Journal of Economic Perspectives*, 27(3), 193–212.

Schmitt-Grohé, S., and M. Uribe (2004): "Solving dynamic general equilibrium models using a second-order approximation to the policy function," *Journal of Economic Dynamics & Control*, 28, 755–775.

Smith, J. A. A. (1993): "Estimating Nonlinear Time-Series Models Using Simulated Vector Autoregressions," *Journal of Applied Econometrics*, 8, Supplement: Special Issue on Econometric Inference Using Simulation Techniques, S63–S84.

Swanson, E. (2012): "Risk Aversion and the Labor Margin in Dynamic Equilibrium Models," *American Economic Review*, 102(4), 1663–1691.

Table 1: The New Keynesian Model: The Structural Parameters

β	0.99	α	0.75
h_{ss}	0.33	ρ_R	0.80
ϕ_1	2.00	κ_π	1.50
ϕ_2	2.00	κ_y	0.125
κ	2.00	π_{ss}	1.00
δ	0.025	ρ_a	0.95
θ	0.36	σ_a	0.006
η	6.00		

Table 2: The New Keynesian Model: Accuracy on Grid

The RMSEs are computed based on $\log\left(z_t/z_t^{true}\right) = \hat{z}_t - \hat{z}_t^{true}$, where $z_t \equiv \left\{c_t, i_t, \pi_t, x_t^2\right\}$ and the true solution is given by the projection approximation. The grid is constructed using 20 points uniformly spaced along each dimension of the state space, giving a total of $20^4 = 160,000$ grid points. The bounds for the interest rate, capital, and technology in the grid range from -3 to +3 standard deviations in a log-linearized solution. For the price dispertion index the grid ranges from -0.005 to 0.05. Bold figures for each of the variables highlight the approximation with the lowest RMSE.

	Standard Perturbation:		Perfect foresight	Extended Perturbation:
	1^{st} order	3^{rd} order		3^{rd} order
RMSEs				
Consumption: c_t	0.00253	0.00170	0.00144	**0.00124**
Investment: i_t	0.06813	0.01718	0.00957	**0.00884**
Inflation: π_t	0.00190	0.00058	0.00060	**0.00049**
Auxiliary control variable: x_t^2	0.18741	0.05578	**0.03863**	0.03866

Table 3: The New Keynesian Model: Accuracy in Simulation

The RMSEs are computed based on $\log\left(z_t/z_t^{true}\right) = \hat{z}_t - \hat{z}_t^{true}$, where $z_t \equiv \left\{c_t, i_t, \pi_t, x_t^2\right\}$ and the true solution is given by the projection approximation. The reported means and standard deviations are in percentage deviation from the steady state. The RMSEs, the means, and the standard deviations are computed using simulated paths based of 20,000 observations with a burn-in of 1,000 observations. Bold figures highlight the best performing approximation method(s).

	Consumption c_t	Investment i_t	Inflation π_t	Aux. control x_t^2
RMSEs				
Perturbation: 1^{st} order	0.00263	0.00811	0.00091	0.01284
Perturbation: 3^{rd} order	0.00116	0.00431	0.00043	0.00499
Perturbation: 3^{rd} order, exact s_t	0.00103	0.00415	**0.00038**	0.00401
Perturbation pruned: 3^{rd} order	0.00134	0.00457	0.00049	0.00579
Perfect foresight	0.00137	0.00371	0.00045	**0.00234**
Extended Perturbation: 3^{rd} order	**0.00094**	**0.00362**	**0.00038**	0.00313
Means				
Perturbation: 1^{st} order	0.0007	0.0013	−0.0002	0.0022
Perturbation: 3^{rd} order	**−0.0005**	−0.0004	**0.0001**	−0.0017
Perturbation: 3^{rd} order, exact s_t	**−0.0005**	**−0.0006**	**0.0001**	−0.0021
Perturbation pruned: 3^{rd} order	−0.0004	−0.0001	**0.0001**	−0.0014
Perfect foresight	−0.0001	−0.0004	**0.0001**	**−0.0040**
Extended Perturbation: 3^{rd} order	**−0.0005**	−0.0004	**0.0001**	−0.0022
Projection: 12^{th} order	−0.0012	−0.0028	0.0004	−0.0041
Standard deviations				
Perturbation: 1^{st} order	0.0152	0.0508	0.0058	0.0587
Perturbation: 3^{rd} order	0.0157	0.0520	**0.0060**	0.0611
Perturbation: 3^{rd} order, exact s_t	**0.0158**	**0.0522**	**0.0060**	0.0616
Perturbation pruned: 3^{rd} order	0.0156	0.0518	0.0059	0.0609
Perfect foresight	0.0156	0.0519	0.0059	**0.0624**
Extended Perturbation: 3^{rd} order	**0.0158**	**0.0522**	**0.0060**	0.0621
Projection: 12^{th} order	0.0162	0.0533	0.0062	0.0637

Table 4: Extended Path: The Terminal Condition

All three terminal conditions imply the same RMSEs for the control variables (denoted $\text{RMSE}_{\mathbf{y}}$) using $N = 250$, where N denotes the horizon in the Extended Path. The RMSEs are computed in a simulated sample path of $5,000$ observations. Starting values for the Extended Path are computed from a third-order perturbation approximation. Bold figures highlight the best performing method for a given value of N.

	RMSEs for terminal conditions		
	$\mathbf{y}_{t+N} = \mathbf{y}_{ss}$	$\mathbf{y}_{t+N} = E_t\left[\mathbf{y}_{t+N}^{1st}\right]$	$\mathbf{y}_{t+N} = E_t\left[\mathbf{y}_{t+N}^{3rd}\right]$
Stable perturbation calibration			
$N = 200$	6.41×10^{-9}	1.32×10^{-10}	$\mathbf{1.29 \times 10^{-10}}$
$N = 175$	6.06×10^{-8}	1.25×10^{-9}	$\mathbf{1.21 \times 10^{-9}}$
$N = 150$	5.63×10^{-7}	1.18×10^{-8}	$\mathbf{1.11 \times 10^{-8}}$
$N = 125$	5.22×10^{-6}	1.10×10^{-7}	$\mathbf{9.91 \times 10^{-8}}$
$N = 100$	7.01×10^{-5}	1.04×10^{-6}	$\mathbf{8.59 \times 10^{-7}}$
$N = 75$	5.63×10^{-4}	1.02×10^{-5}	$\mathbf{7.08 \times 10^{-6}}$
$N = 50$	0.0035	1.32×10^{-4}	$\mathbf{5.54 \times 10^{-5}}$
Explosive perturbation calibration			
$N = 200$	2.77×10^{-8}	2.45×10^{-10}	$\mathbf{2.16 \times 10^{-10}}$
$N = 175$	2.71×10^{-7}	6.37×10^{-9}	$\mathbf{3.62 \times 10^{-9}}$
$N = 150$	2.67×10^{-6}	1.44×10^{-7}	$\mathbf{9.49 \times 10^{-8}}$
$N = 125$	2.67×10^{-5}	2.91×10^{-6}	$\mathbf{2.08 \times 10^{-6}}$
$N = 100$	0.0074	6.00×10^{-5}	$\mathbf{4.46 \times 10^{-5}}$
$N = 75$	0.0165	0.0040	$\mathbf{4.83 \times 10^{-4}}$
$N = 50$	**0.0120**	0.0183	0.0197

Table 5: State-Dependent Horizon in the Extended Path

The RMSEs for the control variables are computed using the horizon $N = 200$ as the benchmark in a simulated sample path of $5,000$ observations. The optimal horizon N^* is restricted to the interval from 20 to 200. Starting values and the terminal condition are obtained from a third-order perturbation approximation. The perturbation approximation at third order and the pruned version are computed without the uncertainty correction to get the perfect foresight approximation. The computations are carried out in MATLAB 2014a using an Intel(R) Core(TM) i5-4200 CPU with 2.50 GHz.

	RMSEs	Mean(seconds) per 1,000 draws	Mean(N^*)
Stable perturbation calibration			
Extended Path: $D_{ss} = 0$	0	385	200
Extended Path: $D_{ss} = 0.01$	7.91×10^{-5}	196	87
Extended Path: $D_{ss} = 0.02$	2.50×10^{-4}	136	58
Extended Path: $D_{ss} = 0.03$	3.92×10^{-4}	101	43
Extended Path: $D_{ss} = 0.05$	5.92×10^{-4}	74	29
Extended Path: $D_{ss} = 0.08$	7.43×10^{-4}	62	21
Extended Path: $D_{ss} = 0.10$	7.89×10^{-4}	51	20
Perturbation: 1^{st} order	0.0071	0.004	–
Perturbation: 3^{rd} order	2.87×10^{-4}	0.05	–
Perturbation pruned: 3^{rd} order	5.05×10^{-4}	0.12	–
Explosive perturbation calibration			
Extended Path: $D_{ss} = 0$	0	496	200
Extended Path: $D_{ss} = 0.01$	6.31×10^{-5}	361	100
Extended Path: $D_{ss} = 0.02$	2.00×10^{-4}	263	69
Extended Path: $D_{ss} = 0.03$	3.40×10^{-4}	208	52
Extended Path: $D_{ss} = 0.05$	7.84×10^{-4}	137	35
Extended Path: $D_{ss} = 0.08$	0.0127	75	25
Extended Path: $D_{ss} = 0.10$	0.0176	66	22
Perturbation: 1^{st} order	0.0134	0.004	–
Perturbation: 3^{rd} order	NaN	–	–
Perturbation pruned: 3^{rd} order	0.0072	0.12	–

Table 6: Combining Perturbation and Extended Path: Stable Perturbation Calibration

The RMSEs for the control variables are computed using $N = 200$ and $EE = 0$ as the benchmark in a simulated sample path of $5,000$ observations. The optimal horizon N^* is restricted to the interval from 20 to 200. Starting values and the terminal condition are obtained from a third-order perturbation approximation. The perturbation approximation at third order is computed without the uncertainty correction to get the perfect foresight approximation. The computations are carried out in MATLAB 2014a using an Intel(R) Core(TM) i5-4200 CPU with 2.50 GHz.

		RMSEs	Mean(seconds) per 1,000 draws	Pct of times Extended Path is used
$D_{ss} = 0$	$EE = 0$	0	385	100
	$EE = 0.00005$	3.28×10^{-5}	57	27
	$EE = 0.0001$	6.20×10^{-5}	35	15.3
	$EE = 0.001$	2.38×10^{-4}	1.4	0.36
	$EE = 0.01$	2.87×10^{-4}	0.5	0
$D_{ss} = 0.01$	$EE = 0$	7.91×10^{-5}	196	100
	$EE = 0.00005$	3.65×10^{-5}	33	27
	$EE = 0.0001$	6.24×10^{-5}	18	15.3
	$EE = 0.001$	2.38×10^{-4}	1.0	0.36
	$EE = 0.01$	2.87×10^{-4}	0.5	0
$D_{ss} = 0.03$	$EE = 0$	3.92×10^{-4}	101	100
	$EE = 0.00005$	1.61×10^{-4}	16	27
	$EE = 0.0001$	1.11×10^{-4}	12	15
	$EE = 0.001$	2.38×10^{-4}	1.0	0.36
	$EE = 0.01$	2.87×10^{-4}	0.5	0
$D_{ss} = 0.05$	$EE = 0$	5.92×10^{-4}	74	100
	$EE = 0.00005$	3.33×10^{-4}	11	27
	$EE = 0.0001$	2.38×10^{-4}	9	15
	$EE = 0.001$	2.38×10^{-4}	1.0	0.36
	$EE = 0.01$	2.87×10^{-4}	0.5	0
$D_{ss} = 0.08$	$EE = 0$	7.43×10^{-4}	62	100
	$EE = 0.00005$	4.63×10^{-4}	7	27
	$EE = 0.0001$	3.49×10^{-4}	5	15
	$EE = 0.001$	2.38×10^{-4}	0.7	0.36
	$EE = 0.01$	2.87×10^{-4}	0.5	0

Table 7: Combining Perturbation and Extended Path: Explosive Perturbation Calibration

The RMSEs for the control variables are computed using $N = 200$ and $EE = 0$ as the benchmark in a simulated sample path of $5,000$ observations. The optimal horizon N^* is restricted to the interval from 20 to 200. Starting values and the terminal condition are obtained from a third-order perturbation approximation. The perturbation approximation at third order is computed without the uncertainty correction to get the perfect foresight approximation. The computations are carried out in MATLAB 2014a using an Intel(R) Core(TM) i5-4200 CPU with 2.50 GHz.

		RMSEs	Mean(seconds) per 1,000 draws	Pct of times Extended Path is used
$D_{ss} = 0$	$EE = 0$	0	498	100
	$EE = 0.00005$	0.0052	151	45
	$EE = 0.0001$	0.0058	119	34
	$EE = 0.001$	0.0068	42	5
	$EE = 0.01$	0.0079	27	0.9
$D_{ss} = 0.01$	$EE = 0$	6.31×10^{-5}	361	100
	$EE = 0.00005$	0.0052	101	45
	$EE = 0.0001$	0.0058	82	34
	$EE = 0.001$	0.0068	29	5
	$EE = 0.01$	0.0079	18	0.9
$D_{ss} = 0.03$	$EE = 0$	3.40×10^{-4}	208	100
	$EE = 0.00005$	0.0044	78	45
	$EE = 0.0001$	0.0050	62	34
	$EE = 0.001$	0.0069	18	5
	$EE = 0.01$	0.0080	11	0.9
$D_{ss} = 0.05$	$EE = 0$	7.84×10^{-4}	137	100
	$EE = 0.00005$	0.0050	55	45
	$EE = 0.0001$	0.0061	39	34
	$EE = 0.001$	0.0073	13	5
	$EE = 0.01$	0.0079	8	0.9
$D_{ss} = 0.08$	$EE = 0$	0.0127	75	100
	$EE = 0.00005$	0.0106	31	45
	$EE = 0.0001$	0.0106	28	34
	$EE = 0.001$	0.0127	10	5
	$EE = 0.01$	0.0145	7	1.2

Table 8: Estimation Results for the New Keynesian Model with DNWR

This table reports the estimates from step 2 in our implemention of SMM, with standard errors in parentesis with soft brackets, except when it is not available (n.a.) due to a boundary constraint. The same random numbers with $\tau = 10$ are used across the various approximations. The simulated sample paths for standard perturbation use the pruning scheme of Kim, Kim, Schaumburg, and Sims (2008) at second order and the scheme suggested by Andreasen, Fernandez-Villaverde, and Rubio-Ramirez (2013) at third order. For extended perturbation, the estimates are obtained from a simulated sample path with $D_{ss} = 0.005$, $N_{min} = 20$, $N_{max} = 200$, and $EE = 0.01$, implying that 15.7 percent of the observations in the simulated sample path are computed by the Extended Path. The standard errors for extended perturbation are computed using EE=0.00 to ensure a smooth objective function.

		Panel A: No DNWR			Panel B: With DNWR		
		Standard perturbation		Extended perturbation	Standard perturbation		Extended perturbation
		2^{nd} order	3^{rd} order	3^{rd} order	2^{nd} order	3^{rd} order	3^{rd} order
Preferences	ϕ_2	0.5798 (0.0737)	0.6328 (0.1686)	0.6645 (0.2695)	2.8366 (0.4432)	2.6484 (0.4004)	0.6645 (0.2695)
Wage adj. costs	ϕ	2705 (1114)	3428 (1185)	3211 (3.2172)	1073 (400.8)	5083 (1874)	3211 (3.2172)
DNWR	ψ	$\to 0$	$\to 0$	$\to 0$	3519 (2116)	6386 (1873)	0.000 (*n.a.*)
Price adj. cost	γ	206.7 (44.81)	203.6 (89.62)	191.13 (4.7173)	29.07 (7.687)	39.39 (12.1117)	191.13 (4.7173)
Monetary policy	ρ_R	0.000 (*n.a.*)	0.000 (*n.a.*)	0.0296 (0.2825)	0.8147 (0.0307)	0.8539 (0.0226)	0.0296 (0.2825)
Monetary policy	κ_π	1.1295 (0.1288)	1.0852 (0.1432)	1.1260 (0.0604)	1.6194 (0.2226)	1.8816 (0.1813)	1.1260 (0.0604)
Monetary policy	κ_h	0.0481 (0.0087)	0.0506 (0.0080)	0.0555 (0.0121)	0.0643 (0.0168)	0.0395 (0.0115)	0.0555 (0.0121)
Tech. shock	ρ_a	0.9245 (0.0154)	0.9379 (0.0190)	0.9367 (0.0241)	0.9604 (0.0067)	0.9577 (0.0088)	0.9367 (0.0241)
Tech. shock	σ_a	0.0149 (0.0018)	0.0132 (0.0027)	0.0131 (0.0022)	0.0115 (0.0012)	0.0129 (0.0016)	0.0131 (0.0022)
Preference shock	ρ_d	0.9952 (0.0018)	0.9984 (0.0011)	0.9977 (0.0014)	0.8889 (0.0241)	0.9038 (0.0272)	0.9977 (0.0014)
Preference shock	σ_d	0.0588 (0.0111)	0.0745 (0.0055)	0.0750 (0.0098)	0.0441 (0.0050)	0.0449 (0.0056)	0.0750 (0.0098)
Objective functions	Q_{SMM}^{step1}	2.5389	2.3183	2.3909	0.9477	0.7686	2.3909
	Q_{SMM}^{step2}	0.1111	0.0974	0.1009	0.0883	0.1091	0.1009

Figure 1: New Keynesian Model: Accuracy Plots

Charts in the left column plot the control variables as a function of $\hat{a}_t$, ranging from -3 to $+3$ standard deviations. Charts in the right column report the log10 errors in the control variables using the projection approximation as the true solution. The conditioning level of the nominal interest rate and the capital stock equals -3 standard deviations in a log-linearized solution. The conditional level of $\hat{s}_t$ is 0.04.

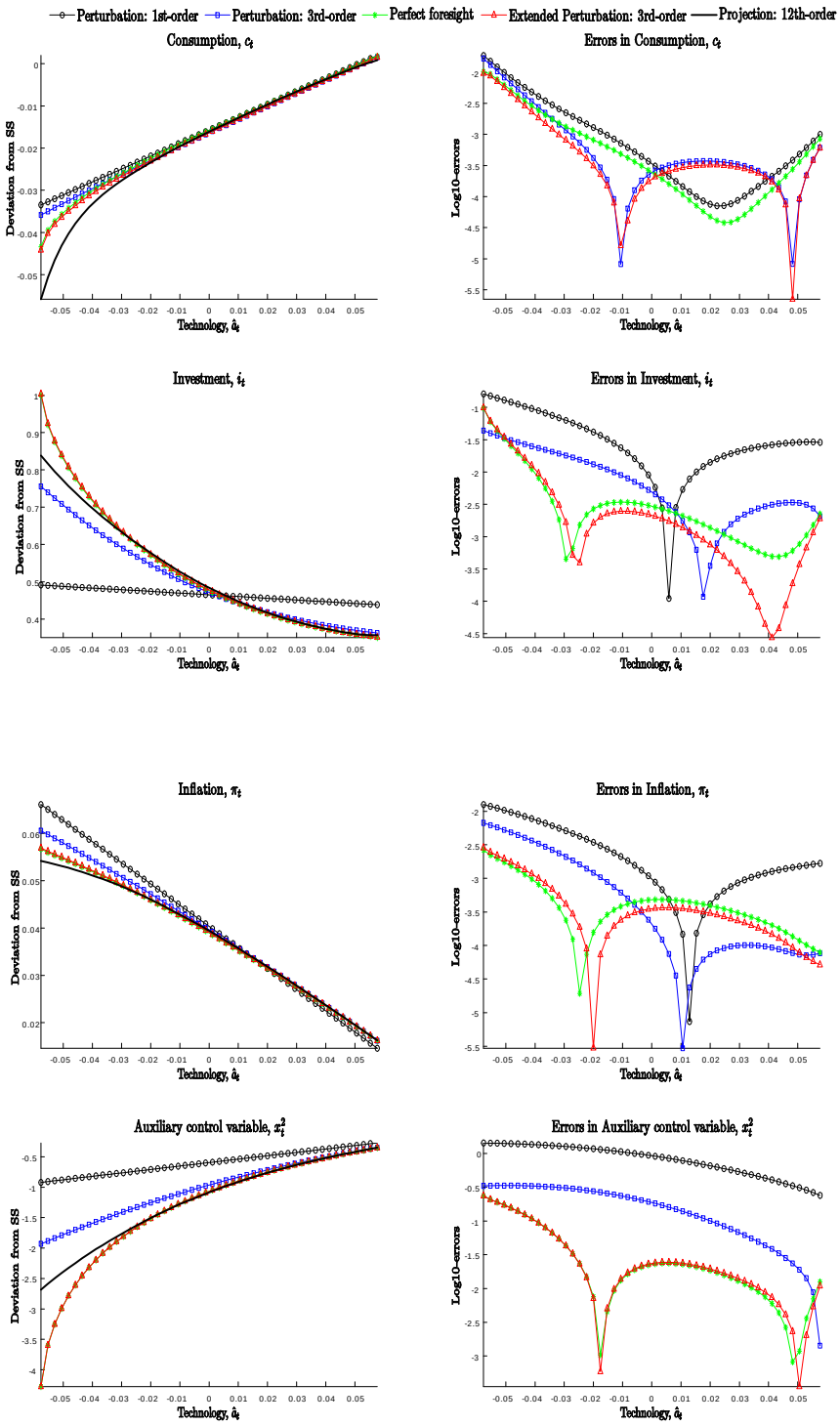

Figure 2: The New Keynesian Model: Stability Plots

The policy function for inflation and the transition function for the price dispertion index are plotted as a function of $\hat{s}_t$. The conditioning level of the nominal interest rate and the capital stock equals -4 standard deviations in a log-linearized solution. The conditioning level of technology equals -3 standard deviations. The histogram for the distribution of $\hat{s}_t$ is computed from a simulated sample path of 20.000 observations using the projection approximation.

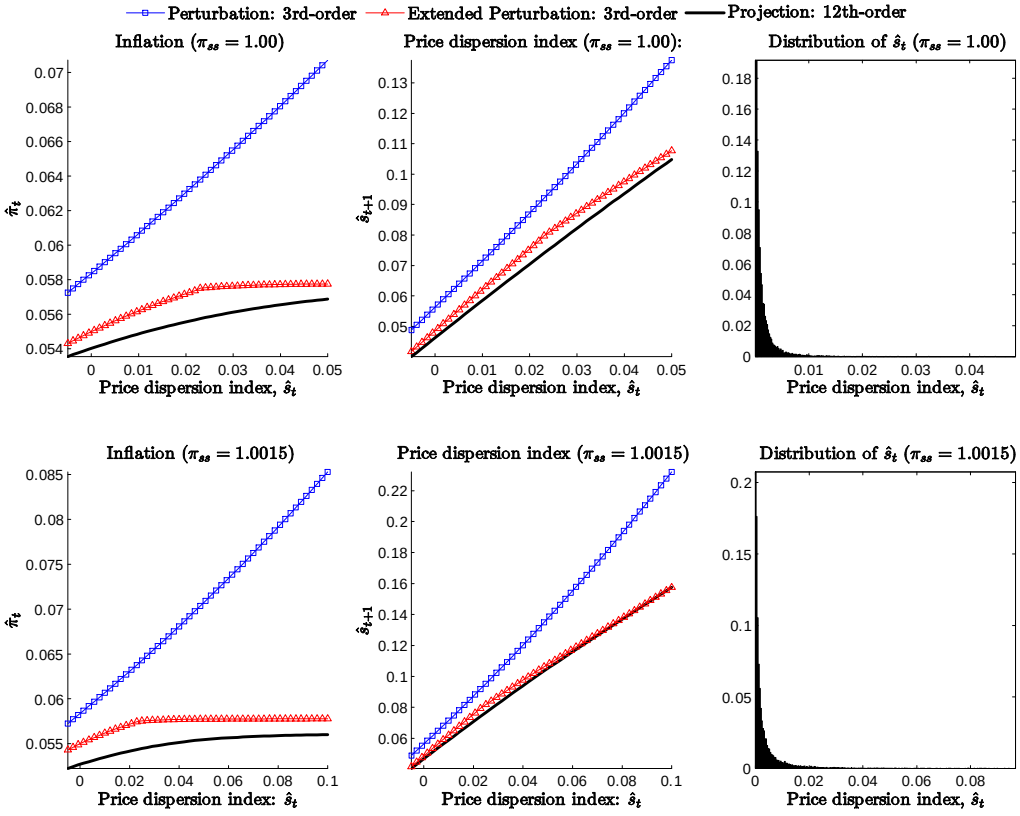

Figure 3: Combining Perturbation and Extended Path: Plot of Sample Path
This figure shows part of the simulated sample where standard third-order perturbation explodes. That is, the simulation is for the explosive perturbation calibration and with $D_{ss} = 0$. The extended perturbation approximation is computed by standard perturbation, except at the areas shaded gray where the Extended Path is used. The y-axis reports the distance of the state variables from the steady state, i.e. $\hat{\mathbf{x}}_t$ from the steady state, i.e. $\|\hat{\mathbf{x}}_t\| = \sqrt{\sum_{i=1}^{n_x} \hat{x}_{i,t}^2}$.

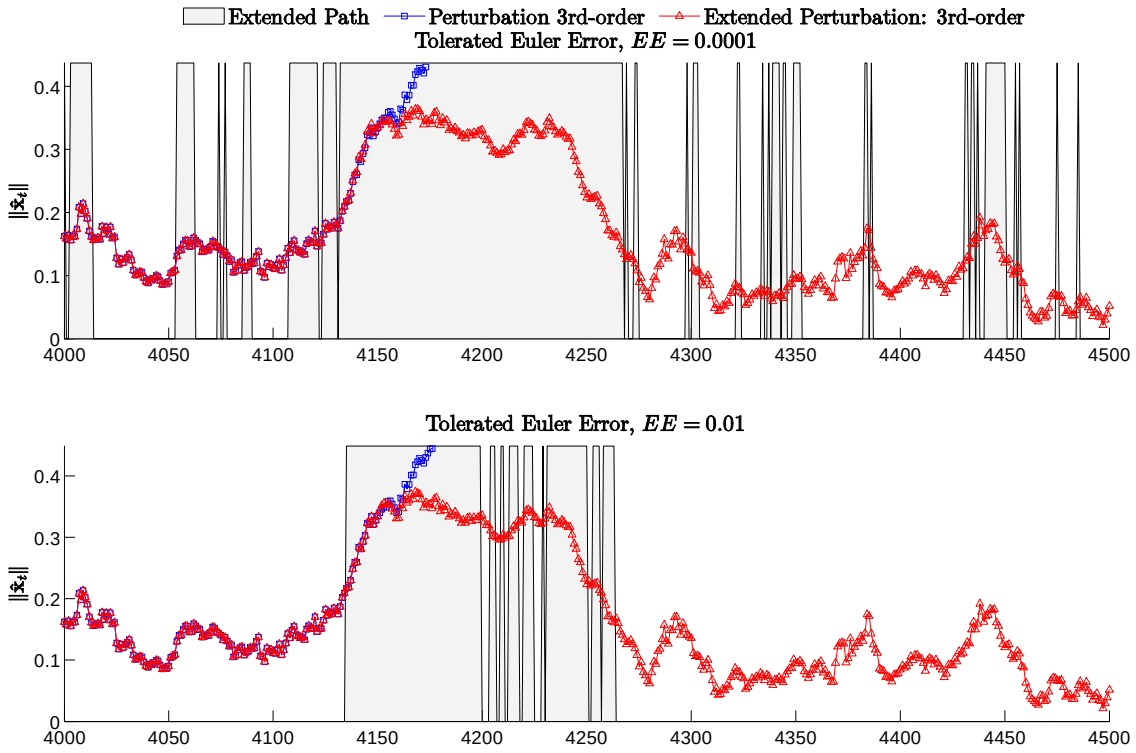

Figure 4: Standard Perturbation: The Asymmetric Wage Adjustment Costs

This figure shows the wage adjustment costs, the marginal costs, and their approximated values which are implied by the estimated parameters for standard perturbation at second and third order as provided in Panel B of Table 8.

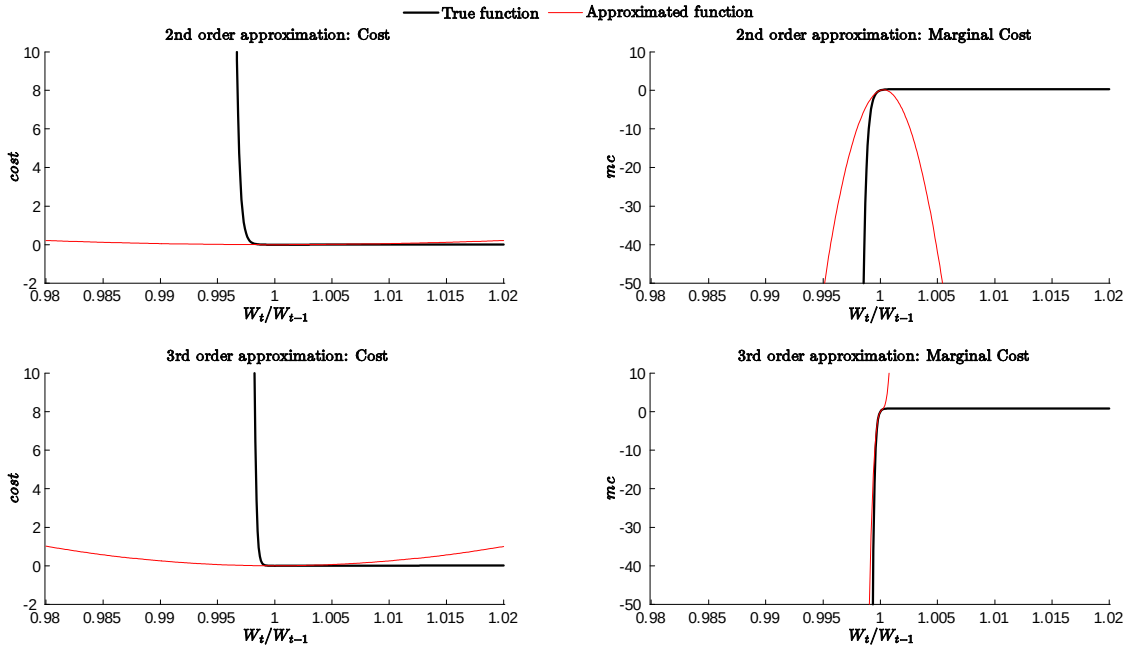

Figure 5: Detrended Nominal Wage Inflation

This figure plots the detrended time series for nominal wage inflation in the U.S. as applied in the estimation of the New Keynesian model.

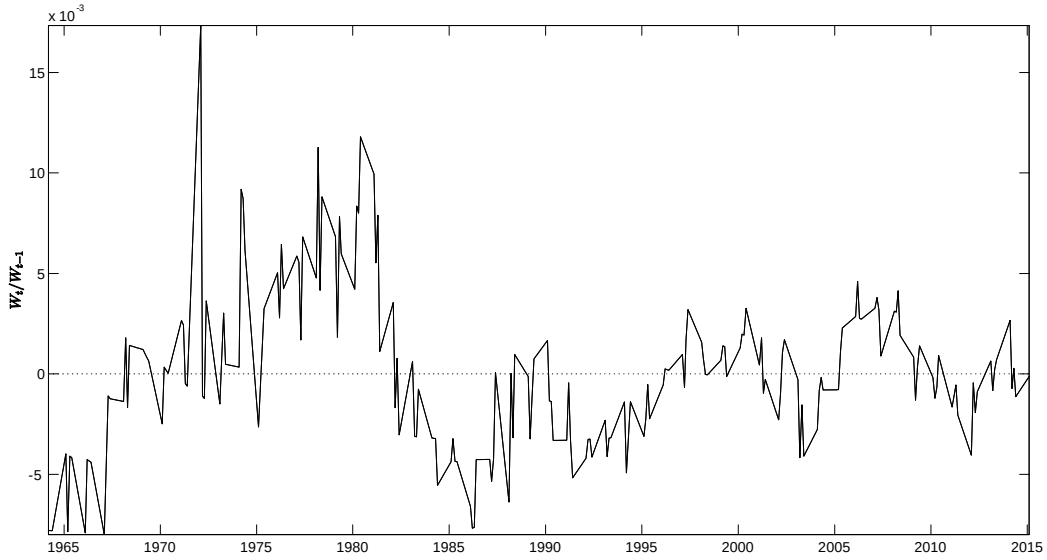

Research Papers 2016

2016-30: Morten Ørregaard Nielsen and Sergei S. Shibaev: Forecasting daily political opinion polls using the fractionally cointegrated VAR model

2016-31: Carlos Vladimir Rodríguez-Caballero: Panel Data with Cross-Sectional Dependence Characterized by a Multi-Level Factor Structure

2016-32: Lasse Bork, Stig V. Møller and Thomas Q. Pedersen: A New Index of Housing Sentiment

2016-33: Joachim Lebovits and Mark Podolskij: Estimation of the global regularity of a multifractional Brownian motion

2017-01: Nektarios Aslanidis, Charlotte Christiansen and Andrea Cipollini: Predicting Bond Betas using Macro-Finance Variables

2017-02: Giuseppe Cavaliere, Morten Ørregaard Nielsen and Robert Taylor: Quasi-Maximum Likelihood Estimation and Bootstrap Inference in Fractional Time Series Models with Heteroskedasticity of Unknown Form

2017-03: Peter Exterkate and Oskar Knapik: A regime-switching stochastic volatility model for forecasting electricity prices

2017-04: Timo Teräsvirta: Sir Clive Granger's contributions to nonlinear time series and econometrics

2017-05: Matthew T. Holt and Timo Teräsvirta: Global Hemispheric Temperatures and Co–Shifting: A Vector Shifting–Mean Autoregressive Analysis

2017-06: Tobias Basse, Robinson Kruse and Christoph Wegener: The Walking Debt Crisis

2017-07: Oskar Knapik: Modeling and forecasting electricity price jumps in the Nord Pool power market

2017-08: Malene Kallestrup-Lamb and Carsten P.T. Rosenskjold: Insight into the Female Longevity Puzzle: Using Register Data to Analyse Mortality and Cause of Death Behaviour Across Socio-economic Groups

2017-09: Thomas Quistgaard Pedersen and Erik Christian Montes Schütte: Testing for Explosive Bubbles in the Presence of Autocorrelated Innovations

2017-10: Jeroen V.K. Rombouts, Lars Stentoft and Francesco Violante: Dynamics of Variance Risk Premia, Investors' Sentiment and Return Predictability

2017-11: Søren Johansen and Morten Nyboe Tabor: Cointegration between trends and their estimators in state space models and CVAR models

2017-12: Lukasz Gatarek and Søren Johansen: The role of cointegration for optimal hedging with heteroscedastic error term

2017-13: Niels S. Grønborg, Asger Lunde, Allan Timmermann and Russ Wermers: Picking Funds with Confidence

2017-14: Martin M. Andreasen and Anders Kronborg: The Extended Perturbation Method: New Insights on the New Keynesian Model